Rivista Italiana di Paleontologia e Stratigrafia	volume 113	no. 2	pp. 223-255	July 2007

THE LOWER EOCENE RODA SANDSTONE (SOUTH-CENTRAL PYRENEES): AN EXAMPLE OF A FLOOD-DOMINATED RIVER-DELTA SYSTEM IN A TECTONICALLY CONTROLLED BASIN

ROBERTO TINTERRI

Received: September 1st, 2006; accepted: March 5, 2007

Key words: Mouth bars, delta-front sandstone lobes, river delta, hyperpycnal flows, tidal deposits, sigmoidal-cross stratification, falling-stage systems tract.

Abstract. The lower Eocene Roda Sandstone (Figols Group, south-central Pyrenees) mainly consists of mouth bars and delta-front sandstone lobes deposited in a flood-dominated river-delta system. The deposition of these bodies was strongly controlled by an interaction between flood-dominated gravity flows entering seawater, topographic confinement and tidal currents.

The Roda Sandstone is made up of six depositional sequences of different hierarchical order each of which is characterized by a basal deltaic sandstone wedge (R1 to R6) that passes upward into a siltstone and mudstone interval. Each basal deltaic sandstone wedge is composed of three types of facies association and respective facies tract (*sensu* Mutti 1992) that, from proximal to distal zones, are indicated as T1, T2 and T3. These three facies tracts are created by the downcurrent evolution of different types of sediment-laden stream flows entering seawater and related hyperpycnal flows. Their deposits are constituted by three different types of coarse-grained mouth bars and corresponding fine-grained delta-front sandstone lobes. The tidal influence is present in facies tract T3 in the R5 and R6 sandstone units, where the passage between flood-dominated mouth bars and the delta-front sandstone lobes occurs through intermediate facies characterized by different types of sigmoidal-cross stratification whose meaning will be discussed.

The basal deltaic sandstone wedges of Roda sandstone are characterized by a progressive forestepping culminating in the R6 unit that erodes the underlying R5 unit and by an overlying backstepping unit indicated as R7. The erosive surface at the base of R6 unit is interpreted as a sequence boundary that divides the Roda Sandstone into two parts: 1) an underlying highstand systems tract (HST) and falling stage system tract (FSST) (units R1 to R5) and 2) an overlying low-stand delta (the R6 unit) that passes upward into highstand mudstone through a transgressive systems tract represented by the R7 unit.

Riassunto. Le Arenarie di Roda (Gruppo di Figols, Eocene inferiore, Pirenei centro meridionali) sono depositi costituiti principalmente da barre di foce e lobi di fronte deltizio che caratterizzano un sistema di river-delta dominato da piene fluviali. La loro deposizione è controllata principalmente dall'interazione tra flussi gravitativi innescati da piene fluviali che entrano in mare e un confinamento topografico che amplifica l'effetto delle correnti tidali.

Le Arenarie di Roda sono costituite da sei sequenze deposizionali di differente ordine gerarchico ognuna delle quali è caratterizzata da un'unità arenacea basale (da R1 a R6) che passa verso l'alto a depositi pelitici. Ogni unità arenacea basale è costituita da tre tipi di associazioni di facies e corrispettivi facies tract che, dalle zone più prossimali a quelle più distali, sono indicati con T1, T2 e T3. Questi tre facies tract sono originati dall'evoluzione sottocorrente di diversi tipi di sediment-laden stream flows che entrano in mare e dai relativi flussi iperpicnali. Il loro prodotto sedimentario si traduce in tre diversi tipi di barre di foce e nei corrispettivi lobi di fronte deltizio. L'influenza tidale è presente nel facies tract T3, nelle unità R5 e R6, dove il passaggio tra le barre di foce dominate da processi fluviali e i lobi di fronte deltizio avviene attraverso particolari facies intermedie caratterizzate da differenti tipi di stratificazioni sigmoidali il cui significato verrà qui discusso.

Da un punto di vista stratigrafico, le unità arenacee delle Arenarie di Roda sono caratterizzate da un progressivo forestepping culminante nell'unità R6 che tronca la sottostante unità R5 e da una unità retrogradante sommitale indicata con R7. La superficie erosiva alla base dell'unità R6 è interpretata come un limite di sequenza che permette di dividere la successione delle Arenarie di Roda in due parti: 1) una parte inferiore rappresentata da un highstand e un falling stage systems tract tract (unità da R1 a R5) e 2) una parte sommitale caratterizzata da un lowstand systems tract (unità R6) che passa verso l'alto a depositi di highstand attraverso un transgressive systems tract rappresentato dall'unità R7.

Introduction

The Lower Eocene Roda Sandstone crops out in the Isabena Valley in the north-western sector of the Tremp-Graus wedge top basin in the south-central Pyrenean foreland basin (Fig. 1). The Roda Sandstone, which belongs to the Ypresian Figols Allogroup (Mutti

Dipartimento di Scienze della Terra, Università di Parma, Viale G.P. Usberti 157/A, 43100, Parma, Italy. E-mail: roberto.tinterri@unipr.it

et al. 1988, 1994) is the first significant sandstone fill of the Eocene succession in the Isabena valley and one of the best examples of tidal influenced fluvio-deltaic sedimentation in the south-central Pyrenees. The unit is characterized by well-exposed outcrops with very good lateral continuity and is thus suitable for developing advanced sedimentological models. The Roda Sandstone has been studied by many sedimentologists over the last thirty years; however these studies often offered controversial interpretations. For example, the unit was first interpreted as a complex of shelfal sand-waves (Nijman & Nio 1975; Nio 1976) and subsequently, as an ebb-tidal delta by Nio et al. (1984) and Nio & Yang (1991). Later, Puigdefàbregas et al. (1985) interpreted the Roda Sandstone as a tide-reworked fan delta of northern provenance, whereas Mutti et al. (1988) suggested a tide-dominated estuarine deposit. More recently, a detailed stratigraphic model was provided by Crumeyrolle et al. (1992; their attachment 1) who interpreted the Roda Sandstone as a tide- and wave-reworked Gilbert-type delta. This interpretation was also adopted by Lopez-Blanco & Marzo (1998) and Lopez-Blanco et al. (2003) who laid emphasis, however, on the tectonic control.

The renewed interest in the fluvio-deltaic sedimentation of tectonically active basins, and especially the role played by catastrophic fluvial floods and related hyperpycnal flows in such types of physiographic settings (e.g., Milliman & Syvitski 1992; Mulder & Syvitski 1995; Mutti et al. 1996, 2000, 2003; Wheatcroft 2000; Martini et al. 2002) has prompted a re-examination of the Roda Sandstone. In particular Mutti et al. (1996, 2000) suggest that ancient flood-dominated depositional systems in tectonically active basins are essentially built up by a series of inter-gradational depositional systems, the end-members of which are represented by fan-delta systems and river-delta systems. Fan-delta systems consist of residual gravel bars and coarse grained delta-front sandstone lobes with hummocky-cross stratification (HCS) deposited by the transformation of dense inertial flows entering seawater. River-delta systems, on the contrary, are mainly characterized by coarse-grained mouth bars, in which traction structures predominate and fine-grained delta-front sandstone lobes with HCS deposited by sediment-laden turbulent flows entering seawater. This approach led Mutti et al. (1996), to suggest that the Roda Sandstone could be interpreted as a series of tidal-infuenced mouth bars deposited by catastrophic floods entering seawater. A similar conclusion has been recently suggested by Crumeyrolle (2003).

The Roda Sandstone moreover is an excellent example of syntectonic deposit (Mutti et al. 1996; Lopez-Blanco et al. 2003; Eichenseer 2003; Crumeyrolle 2003) in which synsedimentary thrusting and folding influenced fluvio-deltaic sedimentation through the creation of topographic constrictions leading to the enhancement of tidal currents. The different points of view about the genesis of the Roda Sandstone are more probably due to the complex interaction among these various controlling factors. Despite the valuable contributions mentioned above, in fact, it is here considered that the stratigraphic evolution of the Roda Sandstone and especially the facies related to interaction between fluvial-deltaic sedimentation, tidal current and topographic confinement are still relatively poorly understood. For these reasons, based on new field work (Tinterri 1999a), the main aims of this paper are: 1) a new interpretation of the facies associations and related processes through a detailed facies analysis of the Roda Sandstone wedges and 2) a re-examination of the Roda Sandstone stratigraphy in order to provide a new sequence stratigraphy interpretation.

General geologic setting

The main structural features of the Pyrenean thrust-fold belt are shown in Fig. 1A, B. The Pyrenees are a double-vergent orogenic belt formed during late Cretaceous to early Miocene times as the result of a broadly north-south continental collision between the Iberian and European plates (Dewey et al. 1989 with references). The Pyrenean chain can be divided into a northern zone dominated by north-vergent thrusts and folds (North Pyrenean zone) and a southern zone characterized by south-vergent folds and thrusts represented by the Axial Zone basement massif and South Pyrenean cover thrust sheets where the thrust-wedge loading and lithospheric flexure gave rise to an extensive east-west trending foreland basin (Muñoz 1992). The southward thrust propagation and related migration of depocenters, that reached a peak in late Middle Eocene, ended in early Miocene and the post-collisional sedimentation is recorded by the undeformed Miocene fluvial and lacustrine strata of the Ebro basin (Fig. 1).

The relationship between the structural evolution and sedimentation of the southern Pyrenean belt between late Cretaceous and early Miocene time have been discussed by many authors such as Soler & Puigdefàbregas (1970), Seguret (1972), Garrido Megias (1973), Puigdefàbregas (1975), Puigdefàbregas & Souquet (1986), Puigdefàbregas et al. (1992), Mutti et al. (1988; 1994), Muñoz (1992) and Teixell (1996).

The south Pyrenean foreland basin can be seen as an WNW-ESE-stretching elongate feature opening and deepening toward the Atlantic with a geometry strongly affected by the reactivation of WNW-ESE oriented mesozoic extensional features although various roughly N-S oriented transverse structures are present, representing lateral ramps related to the southward propagation

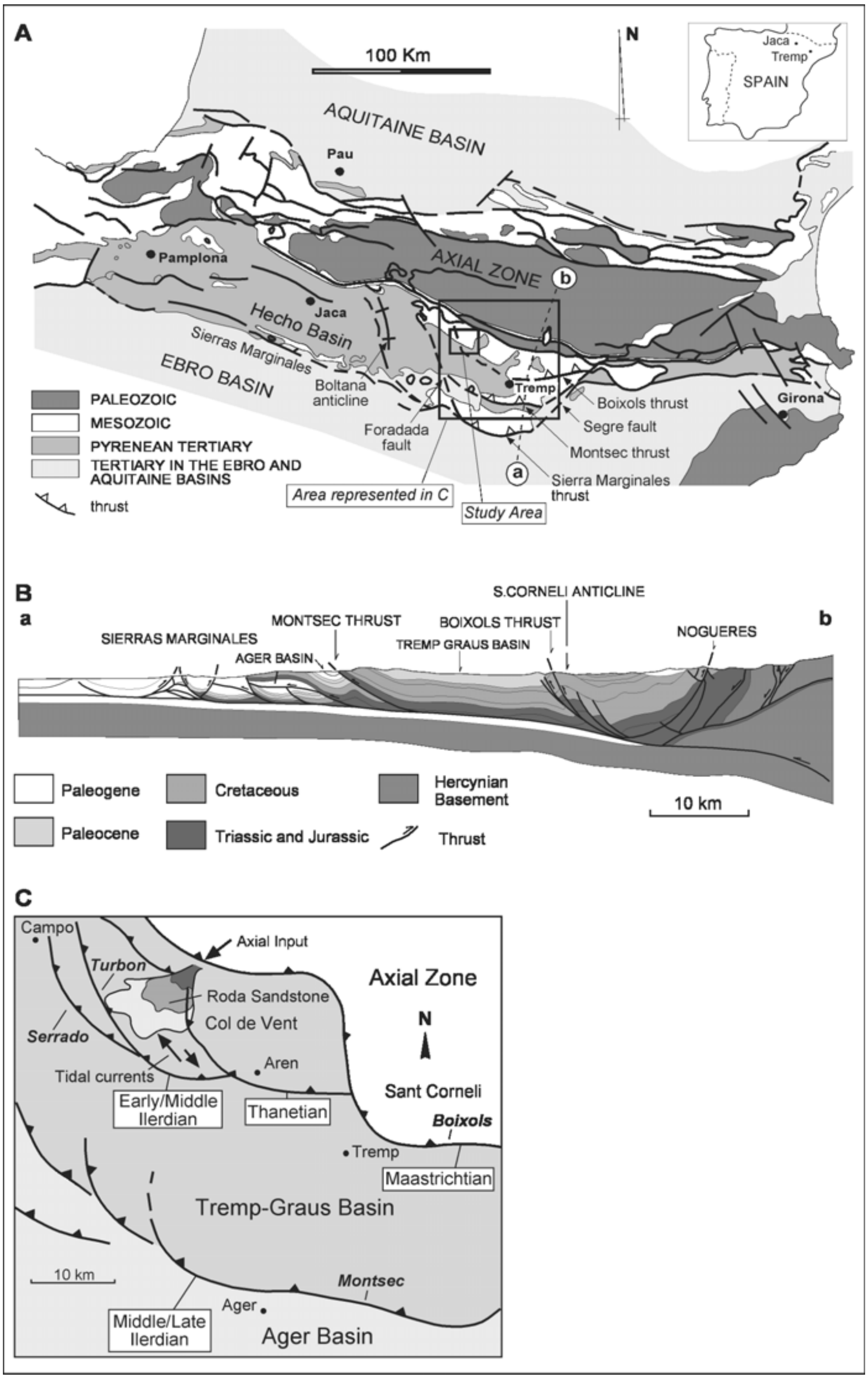

Fig. 1 - A) Geological map of the Pyrenees showing the study area and the main structural elements (redrawn after Remacha et al. 1998). B) Geological cross section of the eastern sector of the Pyrenees (from Puigdefàbregas et al. 1992). C) Paleogeography and structural setting of the study area. The times, in white boxes, indicate the main events of thrust-loading subsidence (slightly modified from Eincheseer & Luterbacher 1992).

of the thrust sheets. These structural features make it possible to identify three sectors characterized by structural settings recording a progressive westward-deepening of the environments: 1) an eastern sector (Tremp-Graus and Ager basins), 2) a central sector (Foradada-Boltana zone) and 3) a western sector (Hecho basin), (Mutti et al. 1988, Fig. 1A). In particular, the basins of the eastern sector, mainly filled with westward and southward-prograding alluvial and fluvio-deltaic deposits, are wedge top basins transported on top of the south Pyrenean central unit (Seguret 1972), which is characterized by three south vergent thrust sheets: from north to south, Boixols, Montsec and Sierra Marginales (Fig. 1A, B). In particular, the Tremp-Graus basin is carried on the Montsec thrust sheet and is bounded to the north and south by the Boixols and Montsec thrusts respectively whereas the Ager basin, carried on the Sierra Marginales thrust sheet, is delimited to the north by the Montsec thrust and to the south by the compressional fronts of the Sierra marginales thrusts. These basins are in turn delimited to the east and west by the Segre and Foradada faults respectively (Fig. 1A) that are interpreted as two transpressive lateral ramps associated to the southward propagation of the south Pyrenean central unit (Mutti et al. 1988).

The main structural features of the study area are shown in Fig. 1C. As pointed out by several studies (Puigdefàbregas et al. 1985; Crumeyrolle et al. 1992; Eichenseer & Luterbacher 1992; Lopez-Blanco et al. 2003), the Roda Sandstone can be seen as a syntectonic deposit mainly controlled by the western extensions of the Boixols and Montsec thrusts (Fig. 1C). These structures controlled not only the geometry of the basin but also the location of the paleovalley from which the fluvial input derived (Puigdefàbregas et al. 1985). The Roda basin is characterized by a roughly NW-SE elongated geometry due to the Roda-Turbon thrust-related anticline that formed a structural high, in the western sector of the studied area. The growth of this curvilinear structure (NNW-SSE to NW-SE, Figs. 1C and 2) which is the western part of the Boixols thrust front and was most likely related to the southward propagation of the Montsec thrust sheet, began in the Paleocene-Early Ilerdian time and continued through all the Ypresian (Lopez-Blanco et al. 2003; Eichenseer 2003). The Roda-Turbon anticline, therefore, separated a deeper water area to the west from a relatively shallower and restricted one to the east where the Roda Sandstone deposition took place. In particular the substantial lack of a time equivalent sandstone deposit in Esdolomada area (log H in Figs 2A, 3) testifies how the deposition occurred mainly in the basin to the east of Roda-Turbon anticline and how this structure represented an important topographic threshold for hyperpycnal flows. Further evidence of this topographic high also includes the development of coralgal reefs in the underlying Alveolina and Puebla de Roda limestone (Carminatti 1992; Eichenseer 2003).

Although the tectonic control before and during the deposition of the Roda Sandstone was already outlined in previous studies (Mutti et al. 1994, 1996; Carminatti 1992; Crumeyrolle et al. 1992; Eichenseer & Luterbacher 1992), only recently the work of Lopez-Blanco et al. (2003) emphasizes the main tectonic structures acting during the deposition of the Roda Sandstone. In particular, based on the integration of seismic and field data, these authors show that the Roda Sandstone is affected by a series of low-amplitude folds, the most important of which, apart from the Roda-Turbon anticline, are: 1) Serraduy syncline, 2) Canerol anticline, and 3) Las Forcas syncline (Fig. 2B). The Roda basin, thus, can be seen as a topographically-controlled basin

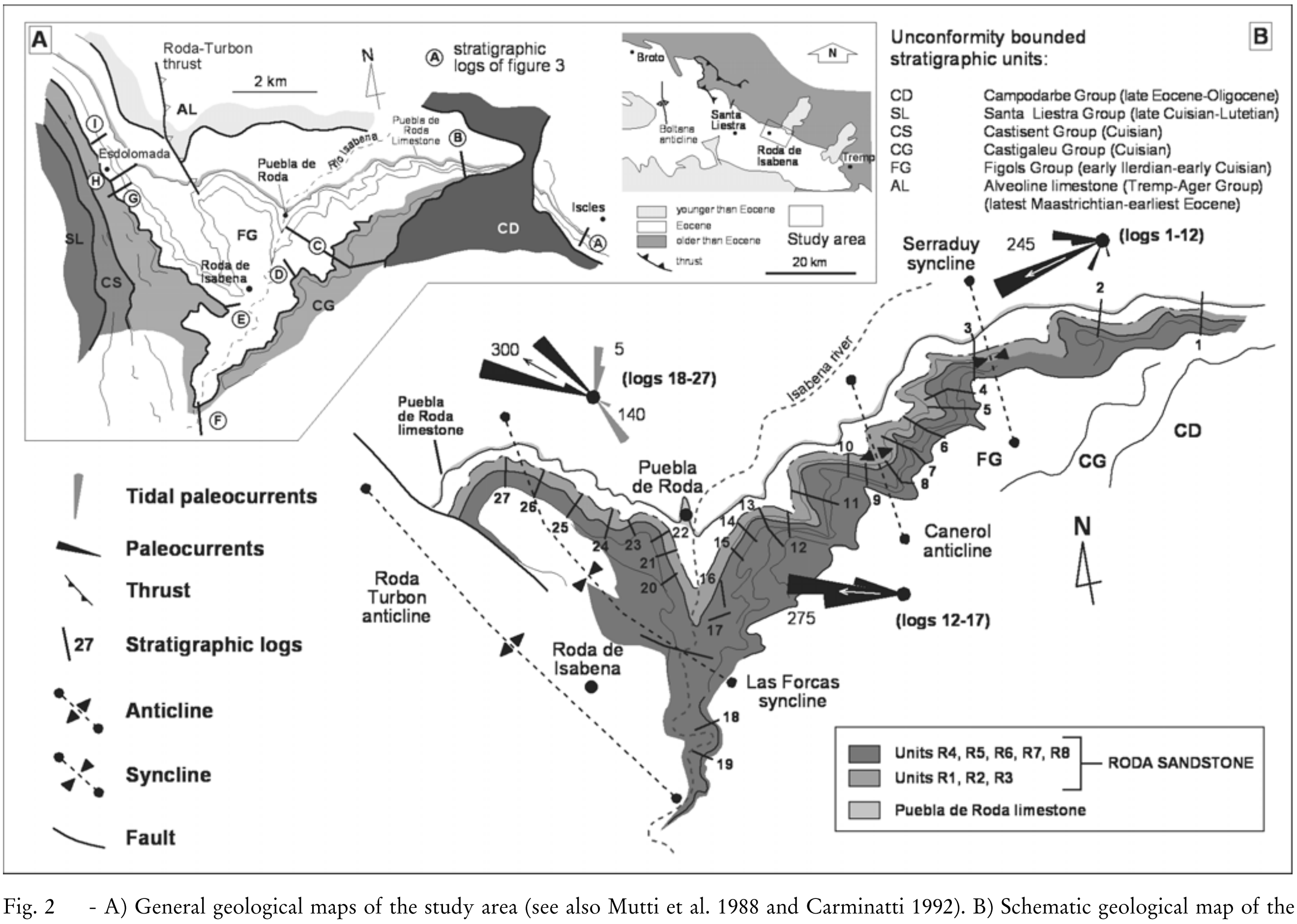

Fig. 2 - A) General geological maps of the study area (see also Mutti et al. 1988 and Carminatti 1992). B) Schematic geological map of the Roda Sandstone in which the Roda folds of Lopez-Blanco et al. (2003) are also indicated.

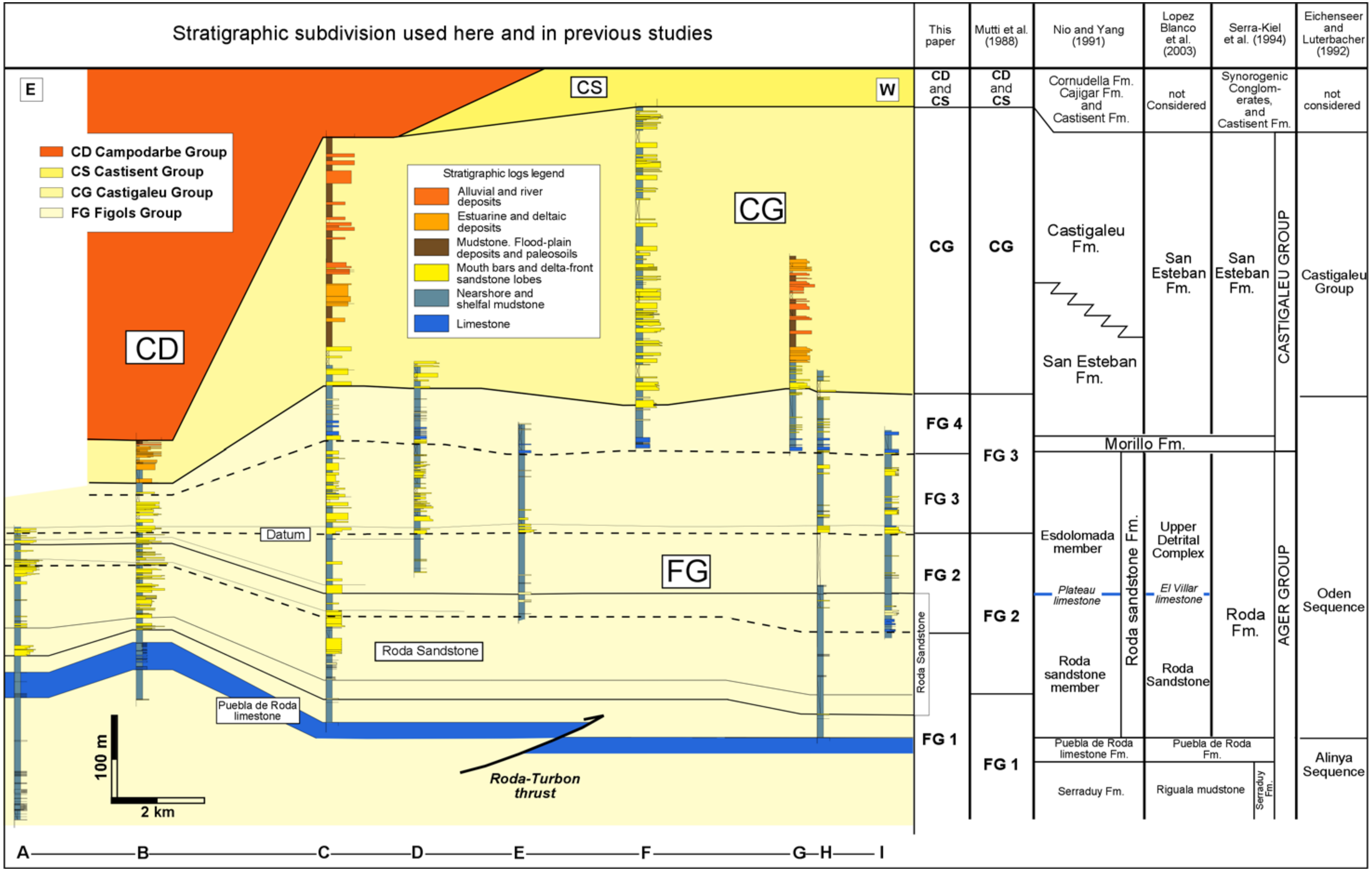

Fig. 3 - General stratigraphic-cross section (see Fig. 2A for the location of stratigraphic logs) in which a comparison between the unconformity bounded stratigraphic units and the main lithostratigraphic units used in previous literature is also shown. See Fig. 2 for the exact location of the Roda-Turbon thrust and related anticline.

characterized by an irregular bottom and confined to the west by the Roda-Turbon thrust-fold.

Finally, the Roda Sandstone is characterized by an arkosic composition (Molenaar et al. 1988) suggesting a main source area in the northern Axial Zone through a tectonically-controlled NNE-SSW oriented paleovalley (Fig. 1C). This paleovalley, probably controlled by the western extension of the Boixols thrust, represents one of the major entry points of the Tremp-Graus basin that was active since the late Paleocene/early Eocene until Oligocene and Miocene with the deposition of the conglomerates of the Campodarbe Group (Puigdefàbregas et al. 1985; Vincent 2001; see also Fig. 3). The arkosic composition of the Roda Sandstone most likely derives from a completely exhumed granitic pluton located a few kilometres northwards of the studied area in the upper Nogueres basement thrust sheet of the Axial Zone antiformal stack (Lopez-Blanco et al. 2003), (see Fig. 1A, B).

Roda Sandstone

• General stratigraphic setting

The term Roda Sandstone derives from the Roda Formation introduced by Mey et al. (1968) to indicate a stratigraphic unit occurring between the Cadi-Alveolina Limestone Formation and the Puente de Montanana Formation. In general, however, the term Roda Sandstone has been used in subsequent literature to denote a terrigenous stratigraphic unit bounded by two shallow-marine carbonate units, i.e. Puebla de Roda limestone and El Villar limestone bed (Fig. 3; Nio & Yang 1991; Crumeyrolle et al. 1992; Lopez-Blanco et al. 2003).

The Roda Sandstone belongs to the Figols Group that is one of the six unconformity-bounded stratigraphic units (allogroups of Mutti et al. 1988, 1994) in which the upper Cretaceous and Tertiary strata of the Tremp-Graus Basin can be divided (Fig. 2). These units, that are recognized and mapped at a basinwide scale, record different and successive stages in the paleogeographic evolution of the Tremp-Graus and Ager Basins related to the southward propagation of the three compressional fronts represented by the Boixols, Montsec and Sierra Marginales thrusts (Fig. 1B).

In particular the Figols Group overlies the Alveolina Limestone, a predominantly carbonate succession characterizing the uppermost part of the Tremp-Ager Group (Upper Thanetian-Lower Ypresian) and underlies the fluvio-deltaic deposits of the Castigaleu Group (Cuisian), (Figs 2A, 3). The Figols Group, investigated in detail by Fonnesu (1984) (see also Mutti et al. 1985, 1988, 1994; Carminatti 1992; Eichenseer & Luterbacher 1992; Barberà et al. 1997; Waehry 1999; Angella 1999 & Calabrese 1999) coincides roughly with the Ilerdian stratotype that Luterbacher (1969) defined in the Tremp area.

The Figols Group was deposited after a major contractional phase that affected the underlying Tremp-Ager Group and that allowed, through the southward propagation of the Boixols, Montsec and Sierra Marginales thrust fronts, the development of two highly subsiding basins represented by the Tremp-Graus and Ager synclines (Fig. 1A, B). In these two basins, the Figols Group represents the first widespread occurrence of siliciclastic sediments in the Eocene succession after the trangressive shallow marine carbonates represented by the classic Alveolina Limestone of Paleocene-Ilerdian age. In this way, the Figols Group records the transition from a predominantly calcareous sedimentation into a predominantly terrigenous sedimentation that characterized the south Pyrenean foreland until the Miocene.

The Figols Group that reaches a maximum thickness of some 1200 m in the western sector of Tremp-Graus basin can be subdivided into four smaller-scale unconformity-bounded stratigraphic units or depositional sequences called Figols 1, 2, 3 and 4 (FG1, FG2, FG3 and FG4, Fig. 3) that record an overall shallowing upward trend related to the southward progradation of fluvio-deltaic systems induced by Boixols and Montec thrust propagation (Fig. 1, 3). The Figols Group was deposited in about 2.7 my (Carminatti & Villa 1993; Barberà et al. 1997) and consequently the duration of each depositional sequence (FG 1, 2, 3 and 4) falls in the range of the 3rd-order cyclicity. Each of these depositional sequences, therefore, records a period of tectonically-induced lowstand of sealevel followed by a period of relative sealevel rise related to tectonic subsidence. As a result, each sequence is characterized by a basal regressive-transgressive wedge of shallow water sandstone that passes upward into a transgressive carbonate-rich facies and highstand mudstone (Mutti et al. 1994). The angular unconformities bounding these units are well expressed especially in Ager basin (Fig. 1A, B); nevertheless high-resolution sequence stratigraphic patterns established for specific sectors of the basin fill make it possible also to trace the four sequences in the Tremp-Graus basin (Mutti et al. 1994; Angella 1999; Calabrese 1999).

The main stratigraphic characteristics of the Eocene succession and thus of the Figols Group in the Isabena Valley are schematically illustrated in Fig. 3 where a stratigraphic interval comprised between the Puebla de Roda Limestone and the alluvial deposits of the Campodarbe Group is shown. In this stratigraphic cross section the large stratigraphic expansion toward the south (see logs B and C) and the progressive angular unconformities due to the propagation of the Boixols thrust front (Fig. 1) can be observed. In Fig. 3 the sequence boundaries are based on those that Mutti et al. (1988, 1994) introduced for this specific zone of the Tremp-Graus basin. They are located along the major angular unconformities, particularly clear in northern sector of the study area (logs A, B and C) that pass along the axis of the Tremp-Graus basin into correlative conformities characterized by forestepping phases of fluvio-deltaic deposits.

In the Isabena valley, the lower boundary of the Figols Group is characterized by an angular unconformity with the uppermost part of the Tremp-Ager Group here represented by the classic Alveolina Limestone. In this zone FG1 is characterized by a relatively deeper sedimentation compared with the Tremp region due to a stronger subsidence that can be related to the Montsec thrust propagation. FG1, in fact, is constituted by a thick shelfal and slope mudstone succession with thin delta-front sandstone lobes indicating a relatively-deep prodelta environment probably recording a lowstand wedge. This, in turn, passes upward into Puebla de Roda Limestone that can be considered as a transgressive deposit capped by a condensed section (Mutti et al. 1988; Nio & Yang 1991).

The stratigraphic succession of the FG1 above the Puebla de Roda limestone mainly consists of mudstone and is characterized, in the upper part, by a laterally continuous bioclastic bed (storm bed of Crumeyrolle et al. 1992) that heralds the passage into fluvio-deltaic deposits of the Roda Sandstone and hence to the FG2 depositional sequence (Mutti et al. 1988, 1994). The Roda Sandstone, in fact, is usually interpreted as the lowstand delta of FG2 characterized by a series of deltaic prograding sandstone wedges showing an overall regressive stacking pattern. These deposits pass upward into highstand mudstone through a relatively thin trangressive systems tract capped by a very distinctive maximum flooding surface (Mutti et al. 1988, 1994) usually indicated as "El Villar limestone bed" (Nio & Yang 1991; Crumeyrolle et al. 1992; Lopez-Blanco et al. 2003) (Fig. 3). The base of FG 3, in turn, is marked by another abrupt increase of terrigenous sediment represented by arenaceous-conglomeratic mouth bars (Fig. 3).

At the top, the stratigraphic succession is truncated by the alluvial conglomerates of the Campodarbe Group, with an angular unconformity that can be recognized at regional scale not only in the Pyrenean chain but also in many other Mediterranean orogens. This unconformity, related to a late Middle Eocene paroxismal phase of thrust propagation coinciding with the Mesoalpine phase in the Alps and Apennines, led to a new paleogeographic organization of the South Pyrenean foreland basin that involved an abrupt southward shift of the main depocenters and the incorporation of a great part of the former foreland basin into the frontal thrust zone.

Sedimentology

• Introduction

The sedimentologic approach used in this paper is based on the process-oriented 'facies tract' concept (Mutti 1992). The facies tract in a flood-dominated fluvio deltaic system is an association of genetically related facies types which record, within each considered system, the downstream evolution of a flood-related sediment gravity flow. The facies concept usually refers to a bedset in the sense of Campbell (1967); nonetheless an ideal facies tract can be seen as recorded by a bed deposited by a single sediment gravity flow undergoing transformations during its basinward motion. In these terms, the concept of gravity-flow facies can be applied to a specific depositional division (i.e. lamina or laminaset, *sensu* Campbell 1967). A facies, therefore, represents the deposit of a gravity flow at a specific location along the path of the flow, whereas a facies tract represents the whole of the facies deposited by a single gravity flow. So, within a bed, the vertical facies association represents how the flow conditions change in time at a fixed location; the horizontal facies association records how the flow conditions change in space through successive flow transformations. This approach implies that, for each considered depositional system, facies tracts must be established on the basis of detailed stratal correlation patterns. For this reason the stratigraphic framework of the Roda Sandstone is based on the detailed measurement and correlation of 27 stratigraphic logs for a total thickness of about 3,2 km (Figs 2B and 4). The Roda Sandstone, moreover, has been inserted in a more regional stratigraphic framework based on the correlation of 9 stratigraphic logs for a total thickness of about 3,3 km (Figs 2A and 3).

Therefore on the basis of the high-resolution stratigraphic framework of figure 4, the Roda Sandstone results as being composed of six fluvio-deltaic conglomeratic-sandstone units (R1-6) that can be traced from coarse-grained proximal zones to finer more distal zones. In particular the R1, R2 and R3 sandstone units can be seen as small-volume coarse-grained units characterized by a well defined facies association indicated as a type 1 deposit (T1 facies tract in Fig. 5A, B). The R4, R5 and R6 sandstone wedges, on the contrary, can be seen as composite bars characterized by a lateral juxtaposition of two different types of deposits, each of which is characterized by a well determined facies association and thus facies tract (Fig. 5). In other words, in the upper sandstone units (R4, R5, R6) proximal type 1 deposits (T1 facies tract) pass upward and downcur-

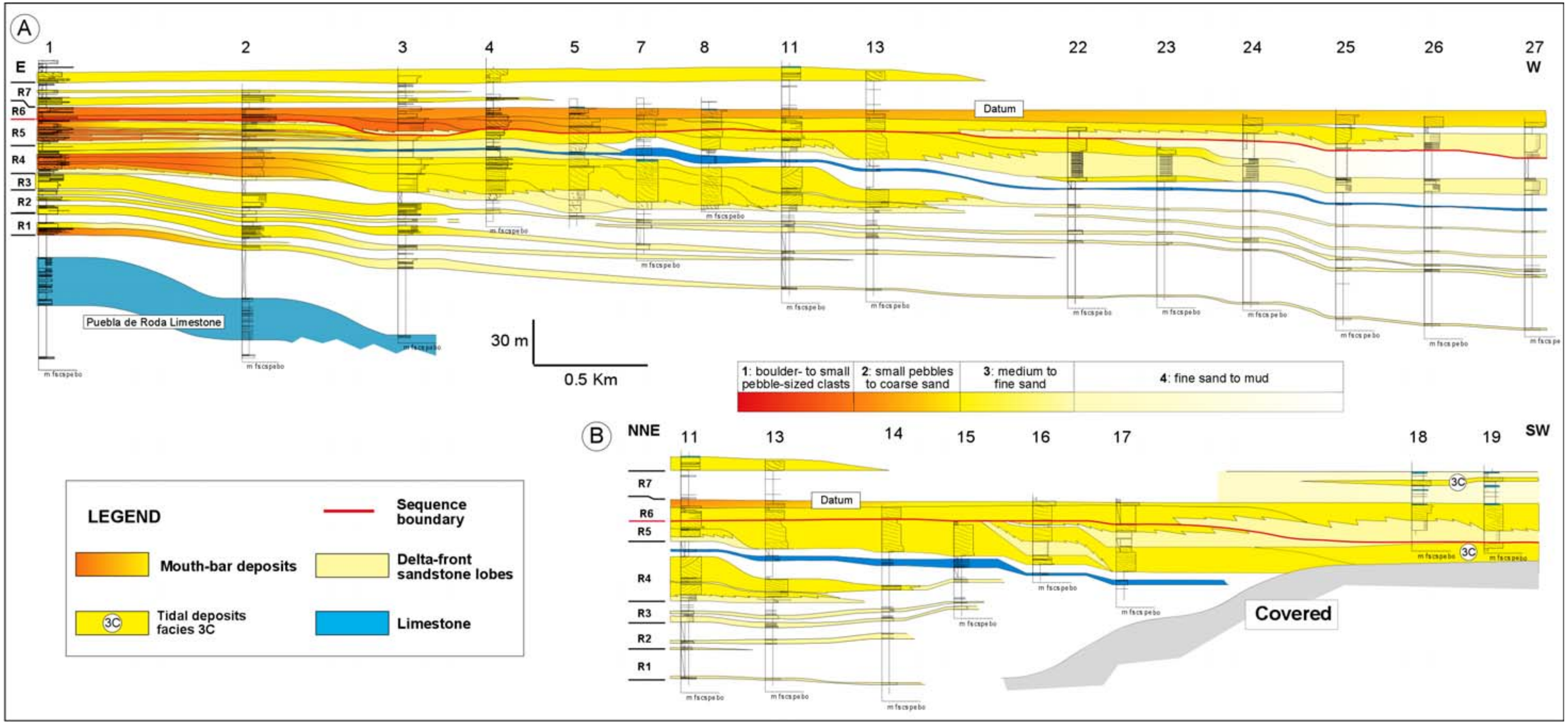

Fig. 4 - Stratigraphic cross sections of the lower Eocene Roda Sandstone (see Fig. 2B for location of stratigraphic logs and traces of the cross sections). On the left, the main sandstone wedges (R1-7) are also indicated. A) Section approximately parallel to the paleocurrents in which very distinctive mouth bar and delta-front sandstone lobe elements can be observed. B) Section approximately perpendicular to the paleocurrents. In the latter the proximal part of the cross section (from log 1 to log 11) is the same of section A and consequently it is omitted.

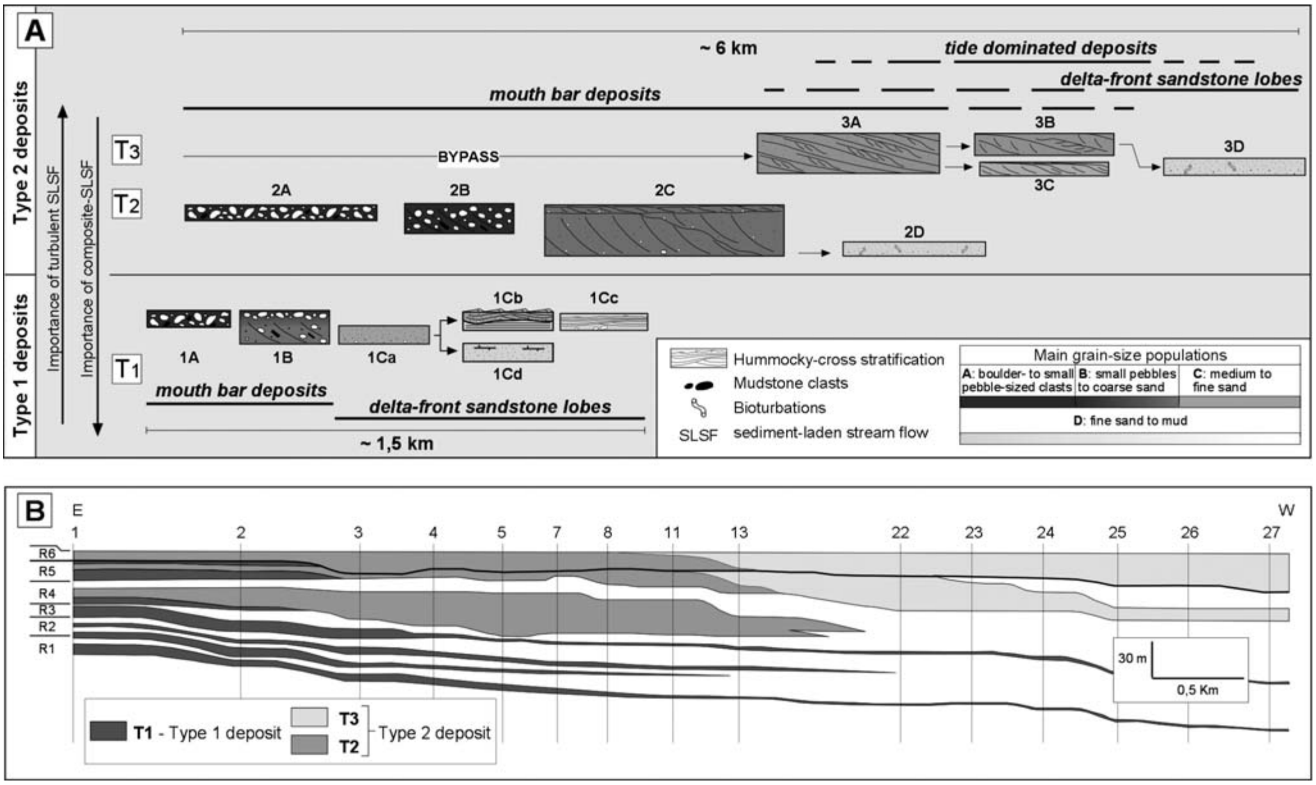

Fig. 5 - A) Diagram showing the three facies tracts (T1, T2 and T3) of the two types of mouth bars and related delta-front sandstone lobes that compose the sandstone units R4, R5 and R6. On the contrary, the R1, R2 and R3 sandstone units are characterized only by type 1 deposits (T1 facies tract). B) Simplified cross section of Fig. 4A showing the distribution of the three facies tracts within the six main sandstone wedges of the Roda Sandstone (see Figs. 2 and 4 for the location of the stratigraphic logs).

rent into another type of deposit of larger volume indicated as a type 2 deposit. The latter is constituted by two facies tracts generated at different times (T2 and T3, Fig. 5; see also Crumeyrolle 2003). In the R4, R5, R6 units, the facies tract T2 is present from log 1 to approximately log 11 for at least 3,5 km, whereas facies tract T3 tends to develop only seaward of log 11 in the R5 and R6 units (Fig. 5B). The R4 unit is the only exception as facies tract T3 is fundamentally absent (Fig. 5B). As mentioned above, each of these three types of deposit (T1, T2 and T3) is characterized by a well defined and complete facies tract that comprises all grain sizes from coarse-grained proximal bars to fine-grained distal sheet sandstone. Therefore, the sandstone wedges R5 and R6 of the Roda Sandstone are interpreted as being built up by at least three facies associations and so facies tracts (T1, T2 and T3), the deposition of which occurred in three successive stages whereas the R4 unit is interpreted as being characterized by only two facies associations (T1 and T2 deposits), the deposition of which occurred in two successive stages (Fig. 5A, B).

• Coarse-grained flood dominated Type 1 deposits

These types of deposit are characterized mainly by coarse grain-size populations and by relatively small volumes. They are situated in the more proximal zones of all the basal sandstone units of the Roda Sandstone and their downcurrent extension is generally less than 1 km (Fig. 5). The macrofossil content is represented mainly by bivalve, gastropods, briozoa, and larger foraminifers. Bioturbation and pebbles and cobbles perforated by lithodomes are common. The facies tract, described in Tab. 1 and Fig. 5A, is essentially composed of three facies 1A, 1B and 1C. The paleocurrents, especially on the basis of facies 1B, indicate flow towards south-west.

The facies described in Tab. 1 stack vertically, generally through erosive boundaries, to form m-thick coarsening upward facies sequences (Figs 6A, B and 7A).

• Interpretation and Discussion of facies tract T1

The interpretation of the facies tract of the proximal coarse-grained deposits is illustrated in Tab. 1 and Fig. 8. The detailed facies analysis of these deposits suggests that they can be subdivided into those related to dense flows (i.e. gravity flows characterised by an interaction of matrix strength, intergranular collisions and excess-pore pressure) and those related to turbulent flows.

The presence, in fact, of matrix- to clast-supported conglomerates with mudstone clasts (facies 1A) indicates deposition by a dense flow, whereas fine-grained laminated facies (facies 1C) can be associated to turbulent sediment gravity flow. Therefore, the type

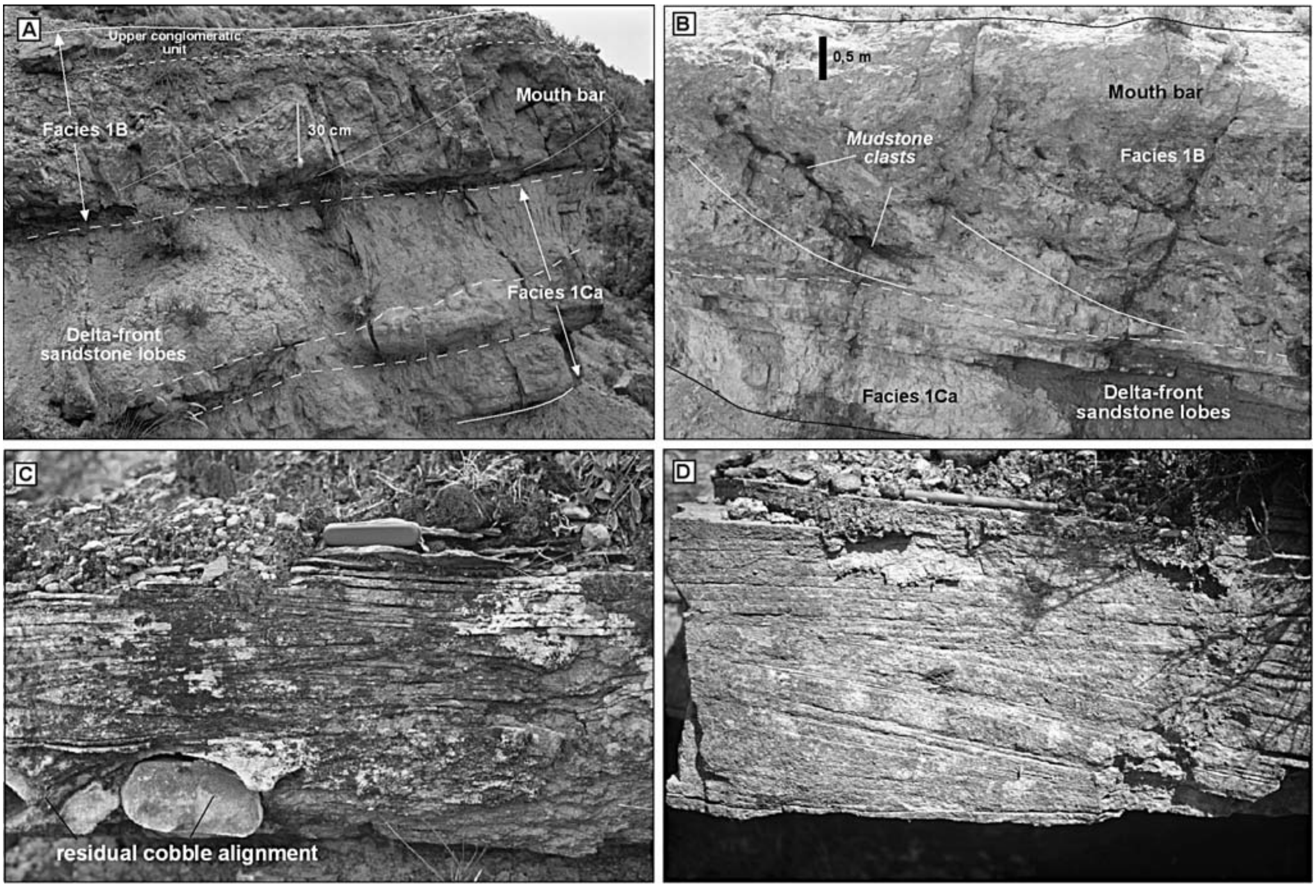

Fig. 6 - Examples of type 1 deposits (T1 facies tract). A and B) facies sequences of type 1 deposits (cf. with Fig. 7A) in the R5 and R4 units respectively (stratigraphic log 1, Fig. 4A). C and D) Examples of hummocky-cross stratification in delta-front sandstone lobes characterizing facies 1Cc (the R4 unit in stratigraphic log 2, Fig. 4A).

1 facies tract can be interpreted as deposited by a subaerial horizontally bipartite sediment gravity flow entering sea water even if a vertical bipartite subaerial gravity flow characterised by a basal inertia carpet cannot be excluded (see Todd 1989).

These types of flow that are observed especially in modern relatively small, high-gradient and gravel-rich alluvial fan systems, are similar to the composite sediment flows of Sohn et al. (1999), and can be considered as hybrid flows characterized by several parts with different mechanical behaviours in which two or more particle-support mechanisms and thus momentum-transport processes can coexist. More precisely, these types of flows, hereafter indicated as composite sediment-laden stream flows (CSLSF, Mutti et al. 2000, 2003), can be seen as a horizontally tripartite flows composed of a frontal dense granular flow followed by an intermediate flow ("turbulent sediment-laden stream flow") and a trailing more dilute-watery flow (stream flow) (Fig. 8). The vertical density-stratified turbulent subaerial gravity flows, on the contrary, are indicated with the term sediment-laden stream flow (SLSF, Mutti et al. 2000, 2003) and in such an environment it cannot be excluded that these flows are able to produce a basal inertia dense flow through liquefaction or bulking processes of the weathering mantle.

At the river mouth, the flow transformation of this type of sediment gravity flow is predominantly characterized by a sudden loss of transport capacity with the possibility of producing a hydraulic jump. This process may cause the freezing of the dense leading edge (facies 1A) and the overtaking, in successive horizontal sedimentation waves or surges, of the more dilute body and tail of the CSLSF (Fig. 8). In particular, the clast-supported conglomerates of facies 1A can be interpreted as recording the deposition of the granular frontal part of the leading edge where the coarser grains are more concentrated, whereas the matrix-supported facies can be interpreted as recording the deposition of the trailing overpressured dense part of the leading edge. Moreover, facies 1B, a traction dominated facies, is interpreted as deriving mainly from traction processes related to the bypass of the body and tail dominated by turbulence. The conglomeratic portion of facies 1B and therefore the traction carpet present at the top of facies 1B can derive from reworking processes of facies 1A and/or from the bedload that characterizes the body of the CSLSF which can also be seen as the tail of the compo-

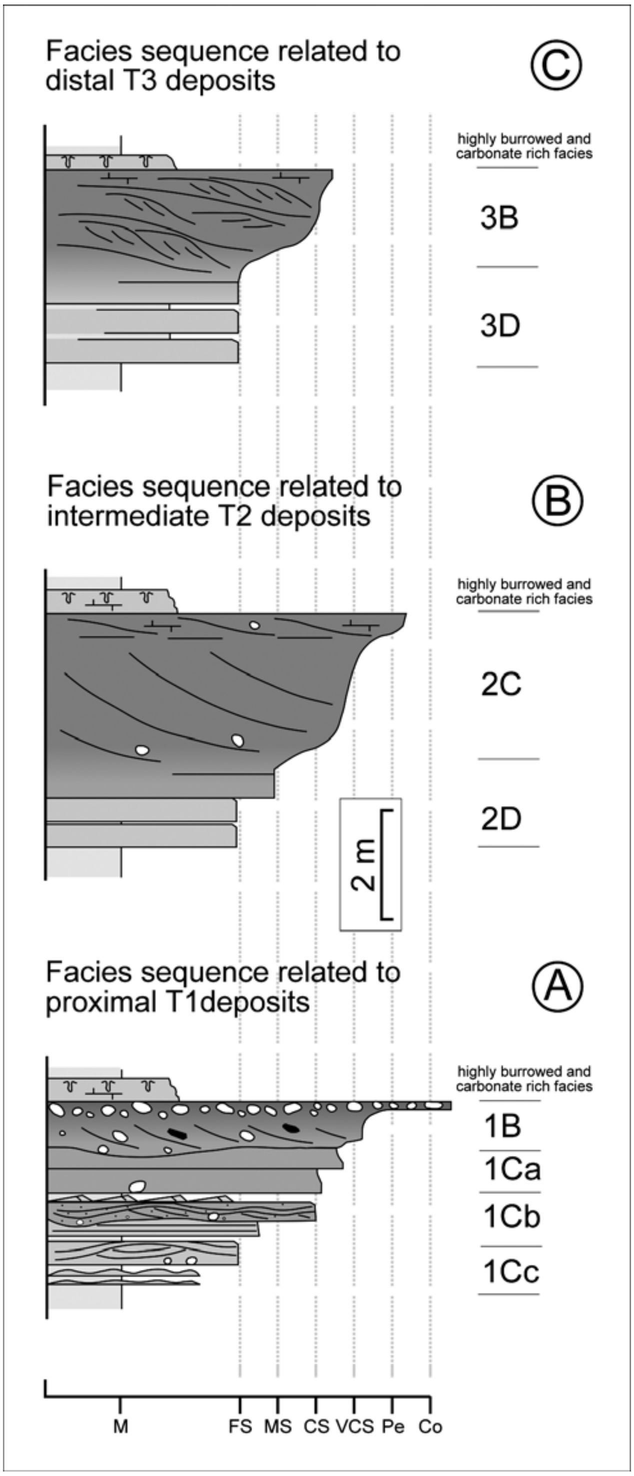

Fig. 7 - Main facies sequences that characterize the three types of deposit that make up the mouth bar and delta-front sandstone lobes of the Roda Sandstone (see Fig. 5A, B).

site leading edge (Fig. 8). Facies 1A and 1B represent the mouth bar facies in sensu stricto.

Facies 1C, on the contrary, is interpreted as delta-front sandstone lobes deposited by hyperpycnal flows derived by the gravitational collapse (cfr. McLeod et al. 1999) of the turbulent body and tail that have overtaken the mouth bar facies. In particular, in R1, 2, 3 units type 1 deposits are mainly characterized by Facies 1Ca, and 1Cd whereas in the upper units they are characterized by Facies 1Ca, 1Cb and 1Cc.

The delta-front sandstone lobes of the lower units, therefore, are lacking in HCS and facies 1Ca pass downcurrent directly into Facies 1Cd where mixed sediments are interpreted as caused mainly by organism colonization that occurs when the fluvial sediment supply is interrupted. During this phase, the substratum, represented by the top of delta-front sandstone lobes, can be enriched with carbonate components transforming the upper part of the deposits into mixed sediment or in some cases into pure carbonate (Molenaar & Martinius 1996). In the upper units, on the contrary, massive (1Ca) and laminated (1Cc) facies are interpreted as depending on the rate of deceleration and so on the lateral expansion of the jet flow, which is a function of the ratio between the flow momentum and water depth at the river mouth (Wright 1977; Mutti et al. 2003). Thus, the massive delta-front sandstone lobes of facies 1Ca could derive from a sudden deceleration that, causing an high rate of fallout, tends to prevent traction processes, whereas the laminated delta-front sandstone lobes of facies 1Cc could be associated with a more gradual deceleration allowing traction processes. Moreover, since facies 1Ca is characterized by grain-size populations coarser than those of facies 1Cc and since these two facies are strictly associated in the facies sequence (see ideal facies sequence of Fig. 7A), it may be suggested that facies 1Ca passes downcurrent into facies 1Cc recording a lateral facies change related to a progressive downcurrent decrease of rate of fallout.

Furthermore, the development of HCS in the upper laminated division of Facies 1Cc (Figs 6C, D), is interpreted as being related to hyperpycnal flows in which the more diluted upper parts experience an oscillatory component. The careful stratigraphic and sedimentological analysis carried out on type 1 deposits (Figs 4, 7A and 8) document that these graded sandstone beds with HCS do not grade upcurrent into beach sediments but into mouth bar facies deposited by flood related CSLSFs entering seawater. Consequently, these sandstones with HCS, even if they are generally considered in the literature as lower shoreface storm beds, are here interpreted as the record of sand-laden density currents, produced by flood events exiting river mouths in which the oscillatory component may derive from several processes like those described in Tab. 2 (see discussions in Mutti et al. 1996, 2003; Tinterri 1997, 2006b and Myrow et al. 2002).

In addition to the normally graded bed with HCS, particular types of composite beds have also been observed. They consist of a series of laminasets with different grain-size populations and sedimentary structures separated by sharp and erosive bounding surfaces,

Facies tract	Facies	Grain-sizes	Thickness	Description	Interpretation	Setting
T1	1Aa	Coarse sand to pebbles and cobbles	Thick to very thick	matrix-supported conglomerate beds characterized by massive to normal grading. Mudstone clasts are also common	Deposition of the trailing overpressured dense part of a composite SLSF leading edge entering seawater (Fig. 8)	MOUTH BAR
	1Ab	Pebbles and cobbles	medium to thick	massive to inversely-graded clast-supported conglomerates. Mudstone clasts are also common	Frictional freezing of the granular leading edge of a composite SLSF entering seawater (Fig. 8)	MOUTH BAR
	1B	Coarse sand to cobbles	Thick to very thick	Inversely-graded cross-stratified pebbly sandstone characterized by a concave upward cross lamination in which tabular mudstone clasts may be present. The top is lined by one or two pebble\cobble-thick traction carpet (Figs. 6A, B)	Traction processes related to the bypass of the body and tail of a CSLSF dominated by turbulence. The conglomeratic portion can derive from reworking processes of facies 1A and/or from the bedload that characterizes the body of the CSLSF which can also be seen as the tail of the composite leading edge (Fig. 8)	MOUTH BAR
	1Ca	coarse to medium sand with cobbles and pebbles	medium to thick	sharp-based massive to normally-graded tabular beds (Figs. 6A, B)	En-masse deposition from sediment-laden hyperpycnal flow (Fig. 8)	DELTA-FRONT SANDSTONE LOBES
	1Cb	fine to coarse sand with pebbles	medium to thick	Composite beds characterized by a series of laminasets with different grain-size populations and sedimentary structures separated by sharp and erosive bounding surfaces, that are vertically stacked to form an inverse to normal grading (Fig. 9A). The coarser laminaset is commonly characterized by erosive bases, hummocky-type structures and residual pebbles very similar to facies (1Cc).	Traction-plus-fallout deposition from sediment-laden hyperpycnal flow characterized by waxing and waning related to the flood hydrograph (Fig. 9B)	DELTA-FRONT SANDSTONE LOBES
	1Cc	fine sand and pebbles	medium to thick	Sharp-based and normally-graded tabular beds chracterized by well-developed HCS. They are constituted by fine sandstone and commonly by a basal conglomerate formed by a one pebble\cobble-thick tration carpet (Figs. 6C, D).	Traction-plus-fallout deposition from sediment-laden hyperpycnal flow in which the more diluted upper parts experience an oscillatory component (Fig. 8, Tab. 2)	DELTA-FRONT SANDSTONE LOBES
	1Cd	Fine sand to silt	thin to medium	massive tabular beds composed of silty to very fine sandstone that can pass downcurrent in mixed sediments in which bioturbation and bioclasts are common	Deposition from dilute sand-laden hyperpycnal flow; mixed sediments are produced by organism colonization that occurs when the fluvial sediment supply is interrupted	DELTA-FRONT SANDSTONE LOBES

Tab. 1 - Description and interpretation of the T1 facies tract (see Fig. 5).

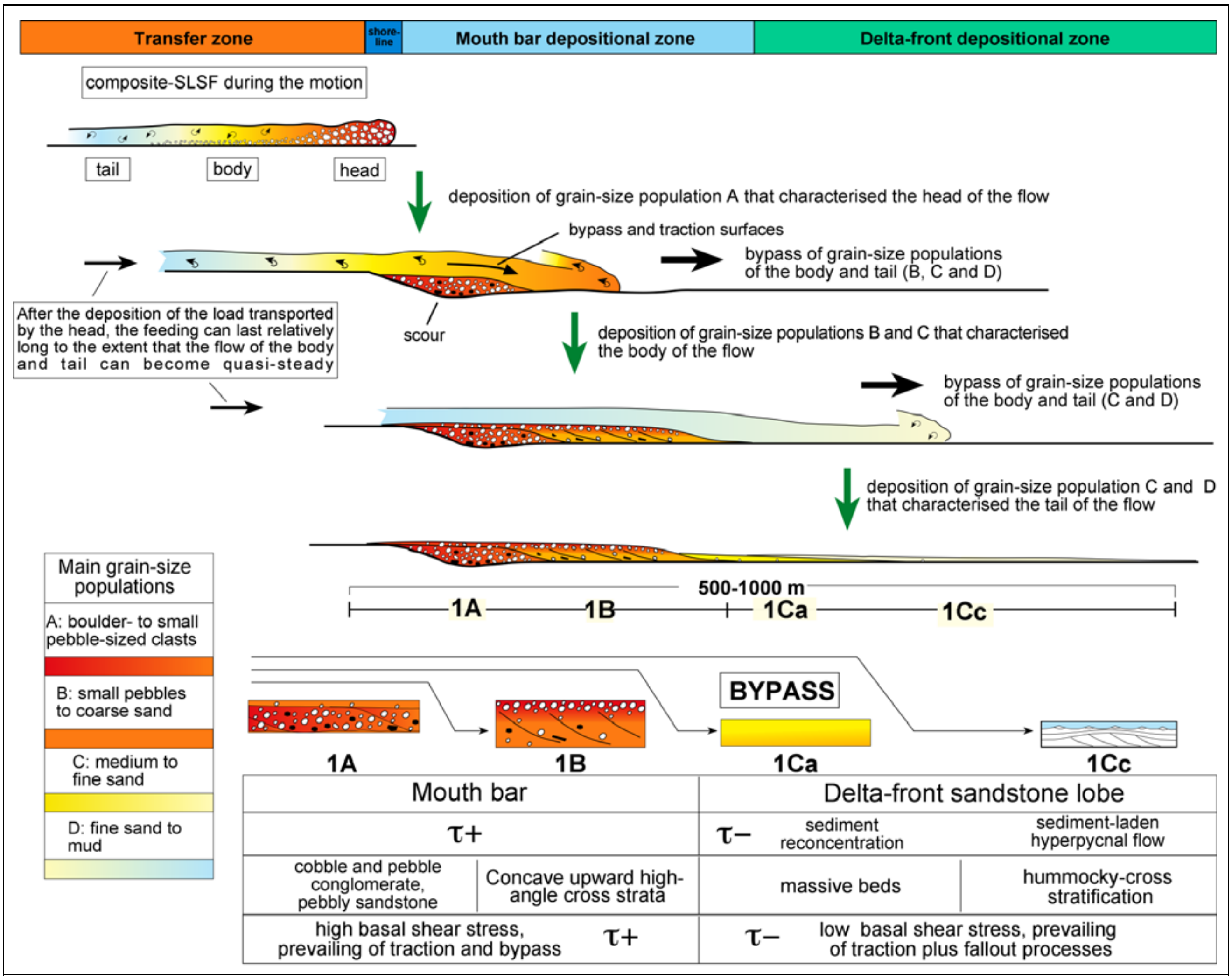

Fig. 8 - Diagram showing the type 1 facies tract deposited by a composite sediment-laden stream flow (CSLSF) entering seawater. The main flow transformations occurring during downslope motion are also shown.

which are vertically stacked in the bed to form an inverse to normally graded strata (facies 1Cb, Tinterri 1999a, b). The coarser laminaset is commonly characterized by erosive bases, hummocky-type structures and residual pebbles similar to facies 1Cc.

In particular, in the case of Fig. 9A, the sandstone bed is composed of four laminasets (A, B, C and D), each of which separated by sharp boundaries and characterized by a distinct grain-size population that increases from A to C and decreases abruptly from C to D. Due to their strictly genetic relationship with mouth bars (Fig. 7A), these types of bed are interpreted as being associated to variations in the steadiness and consequently in flow efficiency of the hyperpycnal flow associated to the flood hydrograph (cf. Mulder et al. 1998). More precisely the laminasets A and B are interpreted as related to the rising limb of the hydrograph whereas laminasets C and D to the peak-flood and falling limb respectively (Fig. 9A), even if unit D could also be interpreted as recording the diluted tail of flood-peak hyperpycnal flow. Although Mulder et al. (1998) have suggested that the vertical grain-size variations related to the rising and falling limb of the hydrograph should be gradual and continuous within the bed, this study documents that they can occur in an abrupt way through erosive boundaries that separate laminasets with different grain-size populations (Tinterri 1999a, b). Recently this type of behaviour has been described also by Mulder et al. (2003).

The presence of these sharp boundaries within the bed probably records the progressive increasing of flow momentum related to the rising limbs of the hydrograph. The volumetric and sediment concentration variations that can occur in these phases can also produce rheological changes within the flow (Best 1992; Wells & Harvey 1987), and evidently the response of the flood-related hypepycnal flow to these changes occurs in a sharp and sudden way through erosive processes. To this purpose, it is interesting to note in the bed shown in Fig. 9A, how a basal erosive surface is well developed, especially in the laminaset C, which is interpreted as being associated to flood peak. The final result will be a delta-

1 - Hydraulic jump at the river mouths, that can be:
a) direct or broken
b) transitional
c) undular

References: Wright and Coleman 1974; Wright 1977; Allen 1982; McLeod et al. 1999

2 - Internal waves at density interfaces within sediment-laden hypepycnal flows

References: Wright et al. 1986; Nemec 1995; Mutti et al. 1996

3 - Surface waves induced by flood entering seawater
a) waves formed at the mouth (flood volume small compared to basin volume)

References: McLeod et al. 1999

b) "sloshing" of sea water (flood volume large compared to basin volume)

References: Mutti et al. 1996

4 - Flow against obstacles (basin margins or topographic highs) and consequent generation of bores (cf. points 1 and 2)

References: Edwards et al. 1994; Kneller 1995

5 - Superimposition of flood-related hyperpycnal flows and storm events
- during storms we have a strong increase in the energy of low frequency waves (infragravity waves)

References: Wheatcroft 2000

6 - Superimposition of flood and tide events
- the flood events can last many hours and days interfering with frequency tides

References: Leithold and Bourgeois 1984; Wright et al. 1986; Nemec 1995

7 - Combination of two or more of the processes mentioned above
- in this case an alternation of low and high group waves due to the interference of oscillations of different frequencies can occur

Tab. 2 - Flow processes able to produce an oscillatory component within an hyperpycnal flow. Some main references are also indicated.

front sandstone bed with an inverse to normal grading in which each laminaset (A, B, C and D, Fig. 9A) will produce a facies tract that becomes finer downcurrent.

In Fig. 9A the correlation pattern between beds I and II was directly observed in the field; the stated correlations with bed III that represents facies 1Cc, were deduced from the analysis of vertical facies stacking as indicated in Fig. 7A. According to the proposed correlation scheme, laminasets A, B tend to pinch out downcurrent, whereas the laminaset C, recorded only by bypass structures in beds I and II, is expected to thicken basinward generating, a single normally graded bed (III) characterized by facies 1Cc consituted by the fine sand that bypassed the proximal and intermediate zones. In other words, the more distal zones are expected to be reached only by the hyperpycnal flows with the highest efficiency (*sensu* Mutti et al. 1999) generated by the flood-peaks (Fig. 9B, Tinterri 1999a, b). As is illustrated in Fig. 9B, the facies sequence of a delta-front sandstone bed depends on where along the depositional profile deposition occurs. In fact, if in the intermediate zone the facies sequence is characterized by inverse to normal grading, in more proximal zones the same sequence could be represented by a bed which is characterized by an internal erosive surface, usually outlined by a residual pebble alignment, indicating the bypass of the hyperpycnal flow related to the flood-peak. Furthermore, in more distal zones the flood event will be recorded by only one normally graded bed related to flood-peak because of its high efficiency and erosive capacity that can erode the deposits related to the rising limb of the hydrograph (Tinterri 1999a, b; see also Tinterri 2006a).

The lateral geometry of a delta-front sandstone lobe associated to a single flood event, therefore, can be very complex, being characterized by erosive and compensation phenomena associated to very low angle progradations and retrogradations that depend on the flow efficiency related to the flood hydrograph. The results of this study support the hypothesis that facies 1Cc is generally downcurrent to facies 1Cb (Figs 5, 9).

Type 1 deposits are thus generated by fluvial-flood events entering seawater without the appreciable intervention of marine-diffusion processes such as waves and tides. The only indication of these processes are represented by pebbles encrusted with oysters and perforated by the lithodomes that can be found especially in facies 1A, indicating that a beach environment likely existed between periods dominated by flood events.

In conclusion, type 1 deposits are interpreted as mouth bars and related delta-front sandstone lobes deposited by CSLSFs in a flood-dominated river delta system.

• Tidally-influenced flood dominated type 2 deposits

The bulk of the deposits of the R4, R5 and R6 units are constituted by a different type of fluvio-deltaic deposits characterized, in comparison with type 1 deposits, by a larger volume. These types of deposit, called type 2, can, in fact, be traced for at least 6 km more

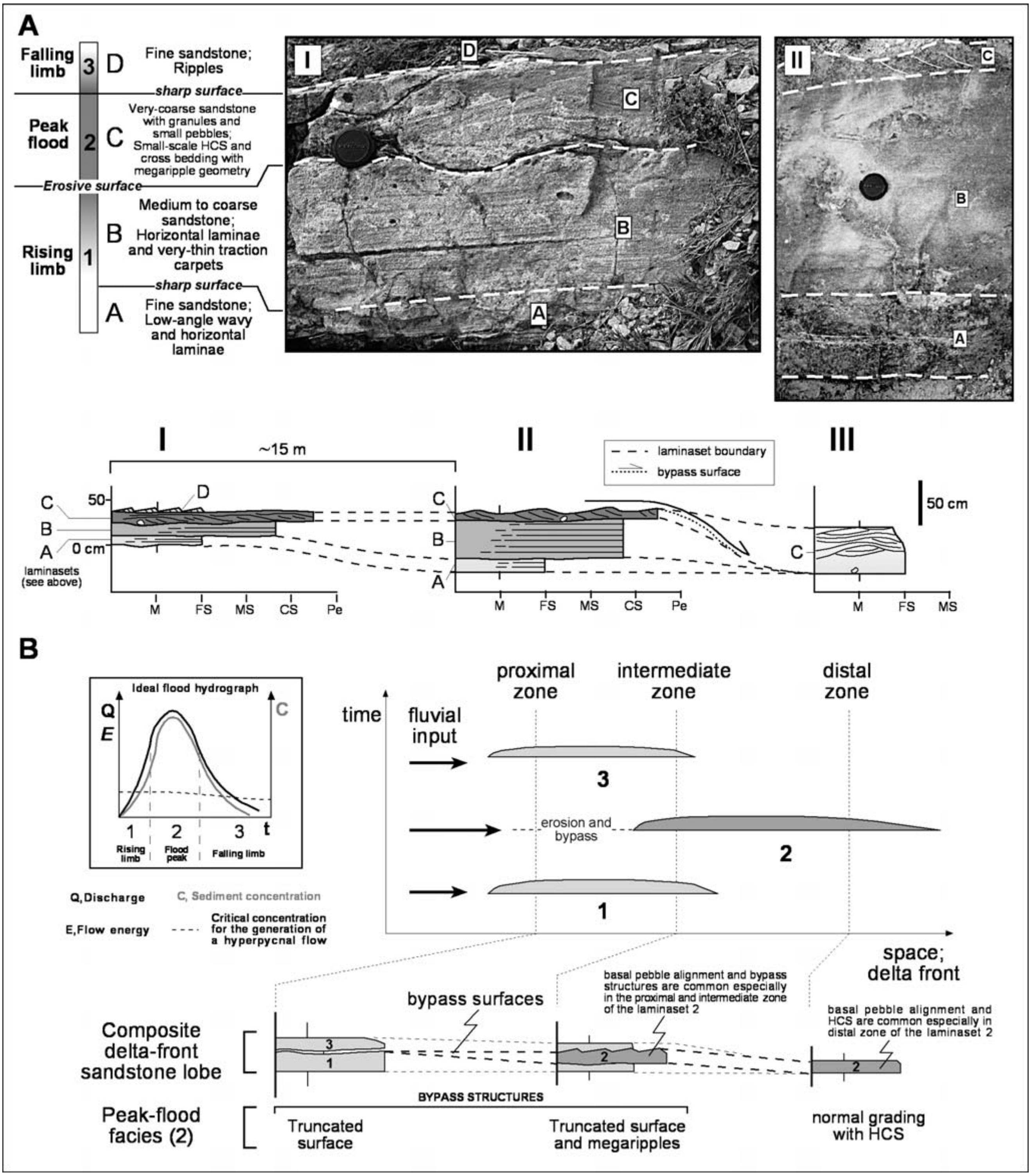

Fig. 9 - A) Example of a composite delta-front sandstone bed (facies 1Cb) characterized by laminasets with different grain-size populations and sedimentary structures separated by sharp and erosive bounding surfaces. The interpretation of the three different phases (1, 2 and 3) related to flood hydrograph are explained in diagram B; lens cap for scale. B) Ideal diagram showing the schematic facies sequences of a delta-front sandstone bed as a function of uniformity and steadiness variations related to flood hydrograph, see text for more details (slightly modified from Tinterri 1999a, b).

basinward than the proximal type 1 deposits (Figs 4A, 5B). The facies tract of this type of deposit is described in Tab. 3 and Fig. 5A.

As mentioned in the introduction, type 2 deposits are formed by two distinctive facies tracts produced in successive periods of time (T2 and T3) (see also Crumeyrolle 2003). Facies tract T2 comprises facies 2A, 2B, 2C and 2D and characterizes predominantly the proximal and intermediate zones of the upper Roda Sandstone units (i.e. R4, R5 and R6 from log 1 to about log

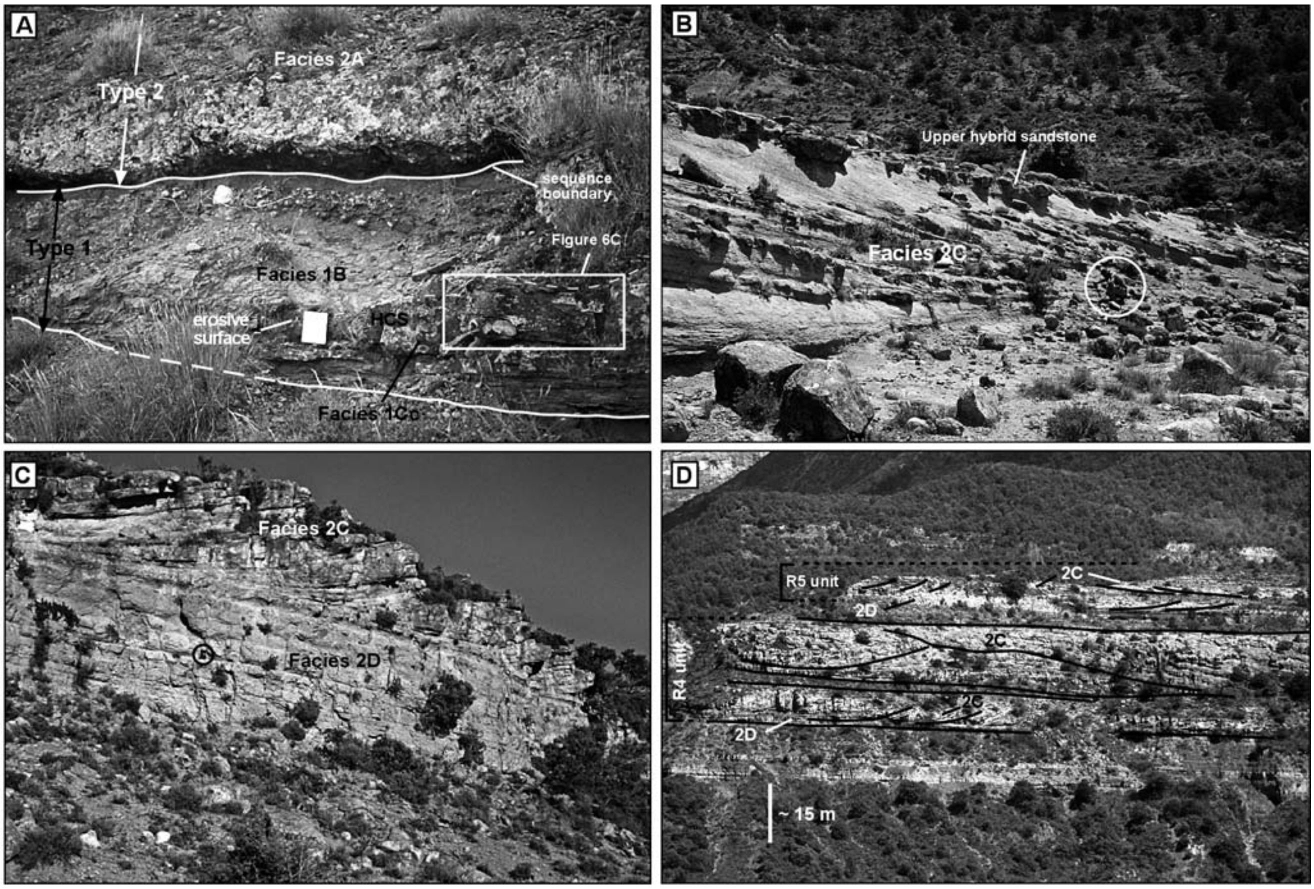

Fig. 10 - A) Erosive boundary between the R5 and R6 units in the proximal zone that also separates type 1 and type 2 deposits (stratigraphic log 2, Fig. 4A). B) Example of facies 2C (R6 unit in log 5, Fig. 4A); encircled person for scale. C) A lateral facies change can be seen between mouth bar of facies 2C and delta-front sandstone lobes of facies 2D (the R5 unit in stratigraphic log 11, Fig. 4); encircled notebook for scale. D) View of facies 2C in which can be noted the passage into delta-front sandstone lobes (facies 2D) and the large-scale concave-upward surfaces that bounded different sandstone unit one hundred meters wide (the cut is approximately perpendicular to the paleocurrents directed toward the reader). For the location see stratigraphic log 11 (Fig. 4).

11, Fig. 5B). Facies tract T3, on the contrary, comprises facies 3A, 3B, 3C and 3D and characterizes the more distal zones of the R5 and R6 units downcurrent to log 11 (Fig. 5B). The only exception is in the R4 unit where facies tract T3 is poorly developed or nearly absent. As in the case of type 1 deposits, the macrofossil content is represented mainly by bivalve, gastropods, briozoa, and larger foraminifers; bioturbation is common in each facies.

Because of the presence of conglomeratic facies 2A, the T2 facies tract has intermediate characteristics between facies tracts T1 and T3 (Fig. 5). In the more distal zone (log 11 in Fig. 4), it is composed mainly of facies 2C that passes downcurrent directly into facies 2D constituted by bioturbated tabular massive beds (Figs. 10C, 10D). The paleocurrents of facies tract T2, on the basis of facies 2B and 2C, indicate flows towards south-west.

In facies tract T3, on the contrary, facies 3A (see Tab. 3 and Fig. 11) passes downcurrent in massive tabular beds of facies 3D (Figs 12, 13D, 14) through intermediate facies characterized by different types of sigmoidal bedding represented by facies 3B and 3C (see Figs 5A, 12). The paleocurrents of facies 3A, on the basis of megaripple and sigmoidal bedforms that characterize the clinoforms, indicate westward flow.

Facies 3C characterizes the R5 unit only (stratigraphic logs 18, 19 in Fig. 4B and logs 17, 21 in Fig. 12) and is constituted by sigmoidal structures (see Tab. 3 and Fig. 13A) very similar to those described in modern environments by Boersma & Terwindt (1981) and in ancient deposits by Mutti et al. (1984, 1985). These sigmoidal units, ranging from a few centimetres to more than one meter in thickness, can be grouped in larger-scale units that can constitute sigmoidal bars of several metres of thickness and several tens of metres in lateral extent (Fig. 13B). Facies 3B, in contrast, characterizes the R5 unit (between logs 13 and 23 of Fig. 4A and between logs 20 and 24 of Fig. 12) and especially the R6 unit seaward of the stratigraphic log 11 (see Fig. 4) and is constituted by another type of sigmoidal bedding which, even if it is apparently similar to that of facies 3C, shows important differences as described in Tab. 3. These two types of facies (3B and 3C) tend to have

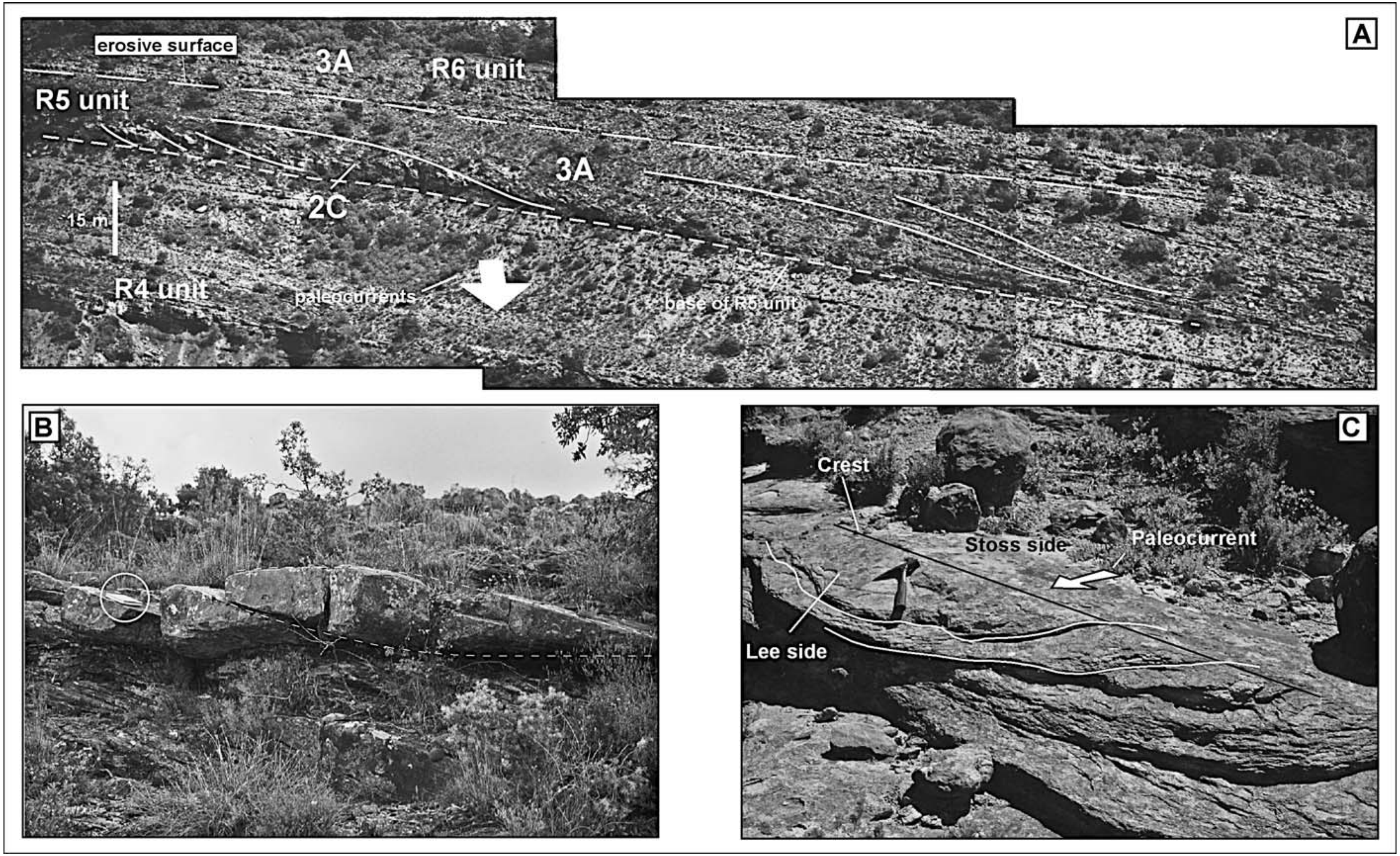

Fig. 11 - Large-scale low-angle sigmoidal clinoforms of facies 3A. The cut is approximately oblique to the paleocurrents (white arrow). In B and C sigmoidal and megaripple bedforms respectively characterizing the large-scale clinoforms are shown. In B, encircled notebook for scale. For the location see logs 13, 14, 15 in Figs 4A, B and 5B.

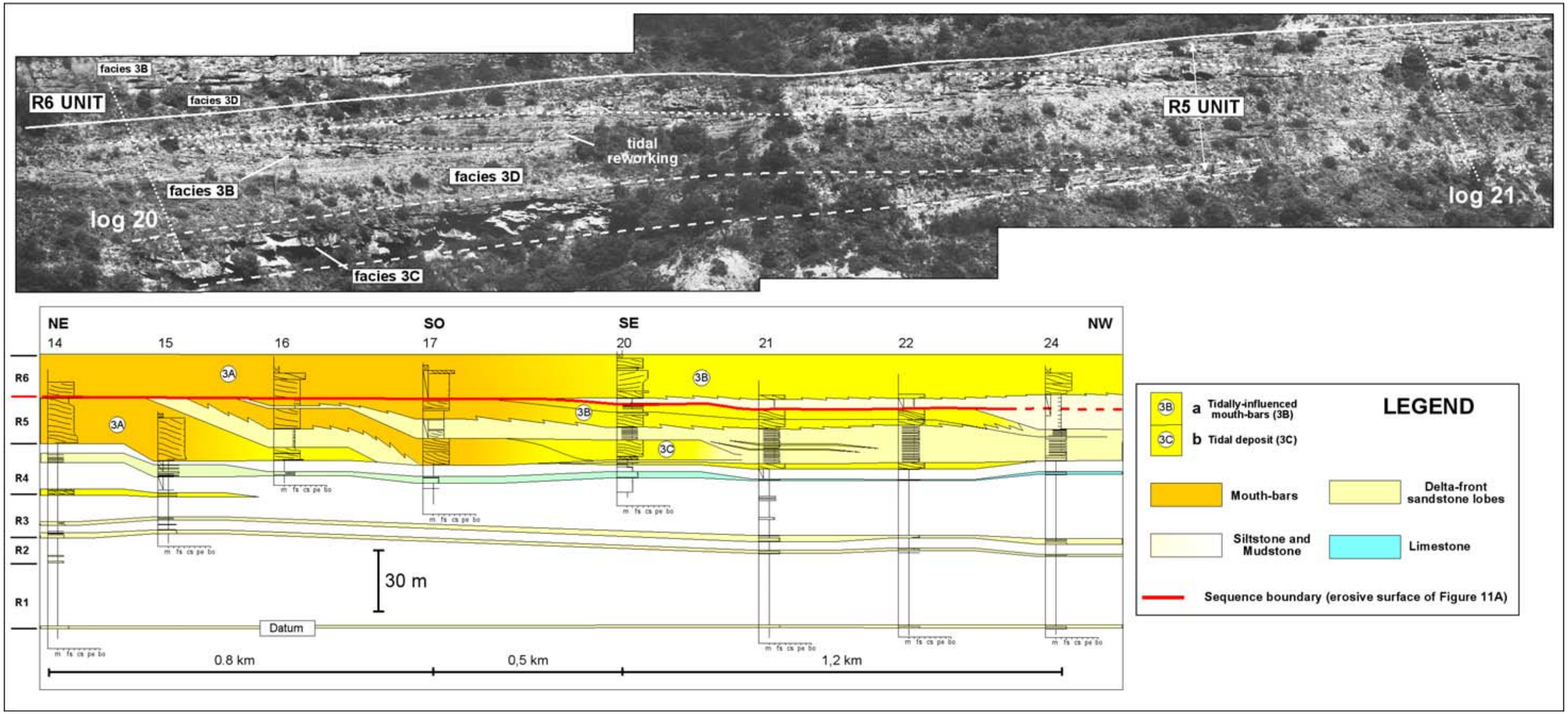

Fig. 12 - View and stratigraphic cross section showing facies change between facies 3B and facies 3D. In the upper view, the cut is approximately oblique to the paleocurrents that are directed toward the page (see Fig. 2B); the location of stratigraphic logs 20 and 21 are also indicated. For the location of stratigraphic logs see Figs 2B and 4.

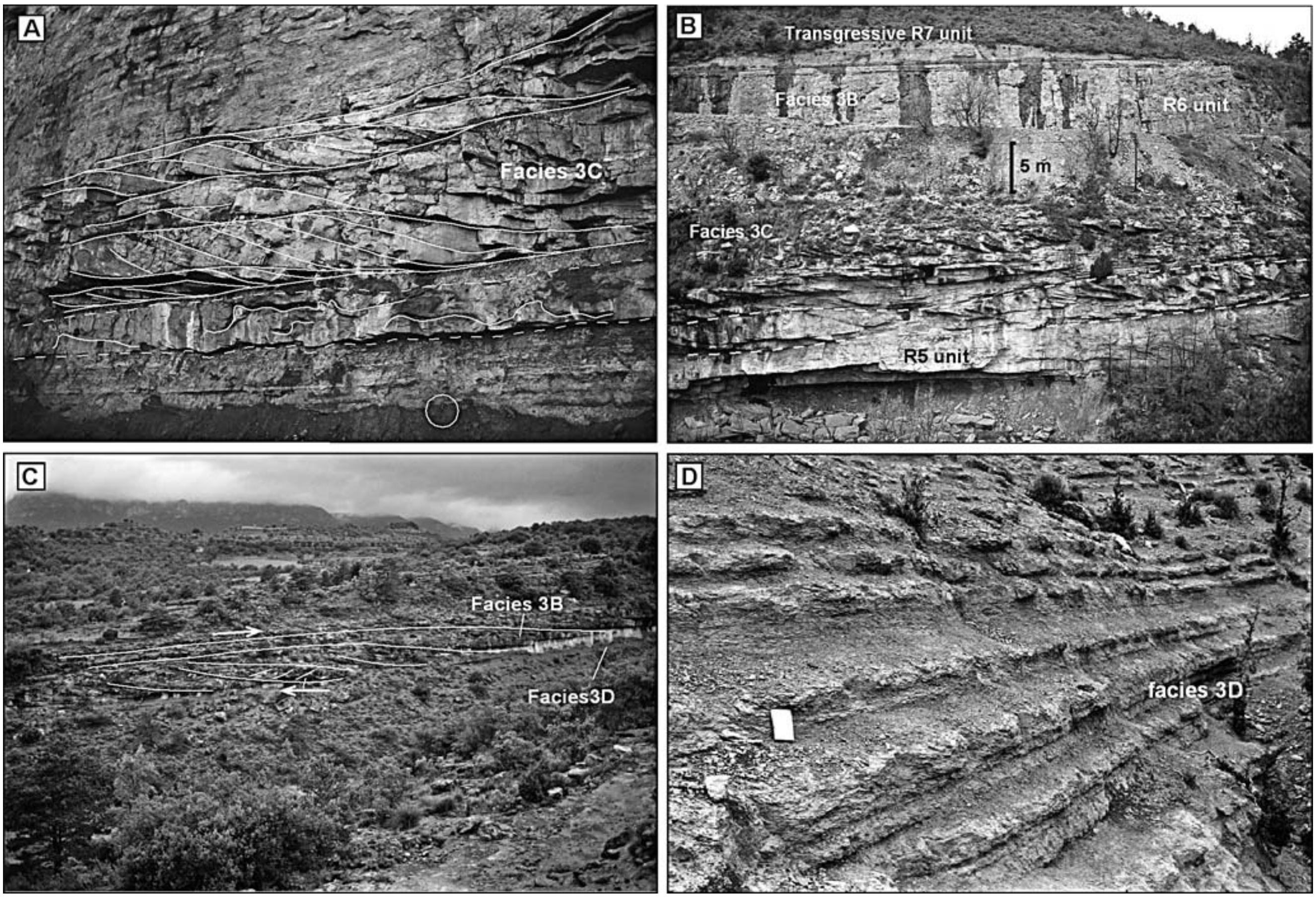

Fig. 13 - Examples of facies 3B, 3C and 3D. A) Tidal sigmoidal bedding of facies 3C in the R5 unit; at the base can be observed a liquefied bed probably related to an earthquake (for the location of outcrop A see log 20 (R5 unit) in Fig. 12; encircled hammer for scale). These bedforms can stack to form high-order stratal units as shown in B located to the south of log 20 (Figs 2B and 12). In C is shown an example of tidally-influenced mouth bar (facies 3B) in the R6 unit, approximately to the west of log 20 (Figs 2B and 12). It is characterized by tidal bedforms directed towards south-east where the lateral passage into facies 3D can be also observed. D) Example of massive delta-front sandstone lobes of facies 3D (the R5 unit, log 24 in Fig. 4).

approximately the same preferential paleocurrent trend directed toward the northwest however, within both facies 3B and 3C, bedforms showing bimodal paleocurrents (toward south-east) are also frequent.

Summarizing, facies tract T3 is characterized by three different types of sigmoidal bedforms represented by facies 3A, 3B and 3C (see Tab. 3).

The facies associations T2 and T3 can stack vertically in m-thick coarsening upward facies sequences as shown in Figs 7B, C respectively.

• Interpretation and discussion of facies tracts T2 and T3

The interpretation of the facies tracts of the type 2 deposits is illustrated in Tab. 3 and in Figs 5 and 15.

Both type 2 facies tracts (T2 and T3) are interpreted as mouth bars and related delta-front sandstone lobes produced mainly by turbulent SLSFs entering sea water; i.e. flood-related gravity flows considered as relatively long-lived density-stratified turbulent flows in which sand and mud are transported as suspended load, whereas the gravel is transported mainly as bed load (basal traction carpet), (Mutti et al. 1996). To support this interpretation for facies tract T2 too (Fig. 5A), notwithstanding the presence of conglomeratic facies 2A that could be easily explained by the deposition of the dense part of a CSLSF, there is the widespread presence of cross bedding in the mouth bar facies (2B, 2C in Fig. 5) indicating how the traction and traction-plus-fallout processes related to a turbulent flow tend to predominate in comparison with the inertia dense flow deposits. For this reason, although in the case of the T2 facies tract some of the SLSFs could be composite (see facies 2A in Fig. 5 and Tab. 3), it is here considered that the vast majority of the gravity flows that deposited T2 and T3 facies tracts, were long-lived density-stratified turbulent flows that, at most, were able to produce a basal inertial flow or modified-density grain flows through the liquefaction processes of the weathering mantle (cf. Todd 1989).

T2 facies tract. In the case of facies tract T2 (Fig. 15), when a composite and turbulent SLSF enters sea

Fig. 14 - View showing the delta-front sandstone lobes (facies 3D) of the R5 and R6 units interpreted as being deposited by flood-related hyperpycnal flows. The outcrop is located between logs 24 and 26 of Figs 4A and 5B.

water, it can be seen as an inertia-dominated outflow because of its density and momentum that can form either axial or plane turbulent jets, depending on the depth of seawater at and seaward of the river mouths (Wright 1977). This phenomenon generates a progressive deceleration and lateral spreading that produces a gravity segregation of the coarser grain-size populations and the bypass of the finer grain-size populations normally segregated within the flow. More precisely, the ratio between the flow efficiency and water depth essentially controls how much flow energy is dispersed at the moment of entering seawater and consequently how much sand is trapped at river mouths and how much sand can escape this region through hyperpycnal flows. In particular, the clast-supported conglomerates of facies 2A can be interpreted as deriving from the freezing of either the basal-granular traction carpet of the SLSF or, possibly, the granular front of a CSLSF leading edge. The matrix-supported facies 2A, on the contrary, can be interpreted as recording the depositions of the overpressured dense part of the leading edge of a CSLSF or of a basal modified-density grain flow of a SLSF. Facies 2B, in the same way as facies 1B, is interpreted as deriving from traction processes related to the bypassing turbulent flow that reworks facies 2A, whereas facies 2C is produced by avalanching processes of the coarse and very-coarse sand that bypass the proximal zone of facies 2A and 2B essentially as bed load, i.e. the large avalanching face described as Gilbert type deltas by Crumeyrolle et al. (1992) (Fig. 15). The concave upward high-angle foresets of facies 2C, with highly tangential geometry, can evolve downcurrent into tabular massive sandstone beds (facies 2D) representing their toesets which can be interpreted as delta-front sandstone lobes (Fig. 10C). Facies 2C, in the same way as the laboratory delta described by Jopling (1965), can be produced because the high velocity SLSF entering seawater can take into suspension a greater proportion of sediment that can be carried beyond the front of the delta. More probably, moreover, this portion of medium and fine sand taken in suspension can collapse generating, as described by McLeod et al. (1999), a sediment-laden hyperpycnal flows that will deposit facies 2D. This facies 2D, however, is present mainly in the more distal zone of facies 2C (R4 and R5 units, Figs 4, 10D). This fact can be explained by the erosive nature of facies 2C, generally organized into units several tens of meters long and bounded up- and downcurrent by erosive surfaces. Figure 10D, for example, shows large-scale units bounded by concave erosive surfaces related to the lateral switching of the main locus of deposition. The coarser sigmoidal megaripples present at the top of the high-angle foresets (see facies 2C, Fig. 5A) are interpreted as bypass structures reworked by the traction of the bypassing SLSF entering seawater.

	Facies	Grain-sizes	Thickness	Description	Interpretation	
T2	2A	Coarse sand to pebbles and cobbles	medium to thick	Matrix and clast-supported conglomerates (Fig. 10A)	Clast-supported conglomerates: frictional freezing of a basal granular traction carpet of a SLSF or of a frontal part of a CSLSF leading edge; matrix-supported facies: freezing of the overpressured dense part of the leading edge of a CSLSF (cf. with Fig. 8) or of a basal modified-density grain flow of a SLSF (Fig. 15)	MOUTH BAR
T2	2B	Pebbles and cobbles	Thick to very thick	Cross-stratified arenaceous-conglomerates that can show an inverse grading	Traction processes related to the bypassing turbulent SLSF that reworks facies 2A	MOUTH BAR
T2	2C	Coarse sand to pebbles	Foresets: very thick Upper bedforms: medium to thick	Large-scale concave upward high angle foresets (> 30°) in which thick laminae with different grain sizes can be recognized (Fig. 10B, C). These deposits commonly pass upward, through a sharp contact, into medium to thick coarser beds particularly rich in bioclasts sometimes characterised by cross-laminae with sigmoidal geometry.	Avalanching processes of the coarse and very-coarse sand that bypasses the proximal zone of facies 2A and 2B essentially as bed load.	MOUTH BAR
T2	2D	Fine sand to silt	Thin to medium	Bioturbated tabular massive beds (Fig. 10C)	High rate of fallout from sediment-laden hyperpycnal flow	DELTA-FRONT SANDSTONE LOBES
T3	3A	medium to coarse sand	Clinoforms: height: about 10-15 m, length: about 100 m. Bedforms: medium to thick	Large-scale sigmoidal clinoforms (Fig. 11A) characterized by megaripple bedforms that can show sigmoidal geometry (Figs. 11B and 16A) and climbing structures (Fig. 11C). Relationship with facies 3D.	Traction and traction-plus-fallout processes related to a SLSF entering seawater, recording the fallout of the coarse and medium sand and the bypassing of fine sand and silt through the formation of hyperpycnal flows. The sigmoidal and megaripple bedforms are bypass structures (Fig. 15).	MOUTH BAR
T3	3B	medium to coarse sand	Clinoforms: height: about 10-15 m, length: about 70 m. Bedforms: medium to thick	Large-scale sigmoidal clinoforms (Figs. 12 and 14) characterized by sigmoidal bedforms. Sigmoidal-cross stratification: in comparison with facies 3C, mud partings and the alternation of thicker sandy and thinner muddy sigmoidal units are absent. The tops are rarely sharp and are commonly characterized by convex geometry with rare climbing structures. Organic fragments and bidirectional structures are present. Relationship with facies 3D (Figs. 13C and 16B)	Traction and traction-plus-fallout processes related to an interaction between a SLSF entering seawater (see facies 3A) and tidal currents (see text for more details). The sigmoidal bedforms are bypass structures (Fig. 15).	MOUTH BAR / TIDAL DEPOSITS
T3	3C	medium sand	medium to thick	Sigmoidal-cross stratification (Figs 13A, B and 16C): offlapping series of sigmoidal-shaped sandstone units separated from each other by thinner silty and clayey partings. Each sigmoidal unit may be internally cross bedded and both the sigmoids and their internal cross bedding grade downward into tangential bottomsets characterized by thin sand and mud laminae; the top is often represented by a sharp erosive surface. The alternation of thicker sandy sigmoidal units and thinner muddy sigmoidal units with mud couplets is well developed (Fig. 16C). No relationship with facies 3D.	Traction and reworked processes related to semidiurnal tidal currents in subtidal environment. The well-developed cyclicity can be associated to neap-spring cycles. Sigmoidal bedforms are subtidal bars.	TIDAL DEPOSITS
T3	3D	Fine sand to silt	Thin to medium	Massive bioturbated tabular sandstone beds with very rare "flaser" type structures composed of organic material (Figs. 13D and 14)	High-rate of fallout from sediment-laden hyperpycnal flow (Fig. 15)	DELTA-FRONT SANDSTONE LOBES

Tab. 3 - Description and interpretation of the T2 and T3 facies tracts (see Fig. 5).

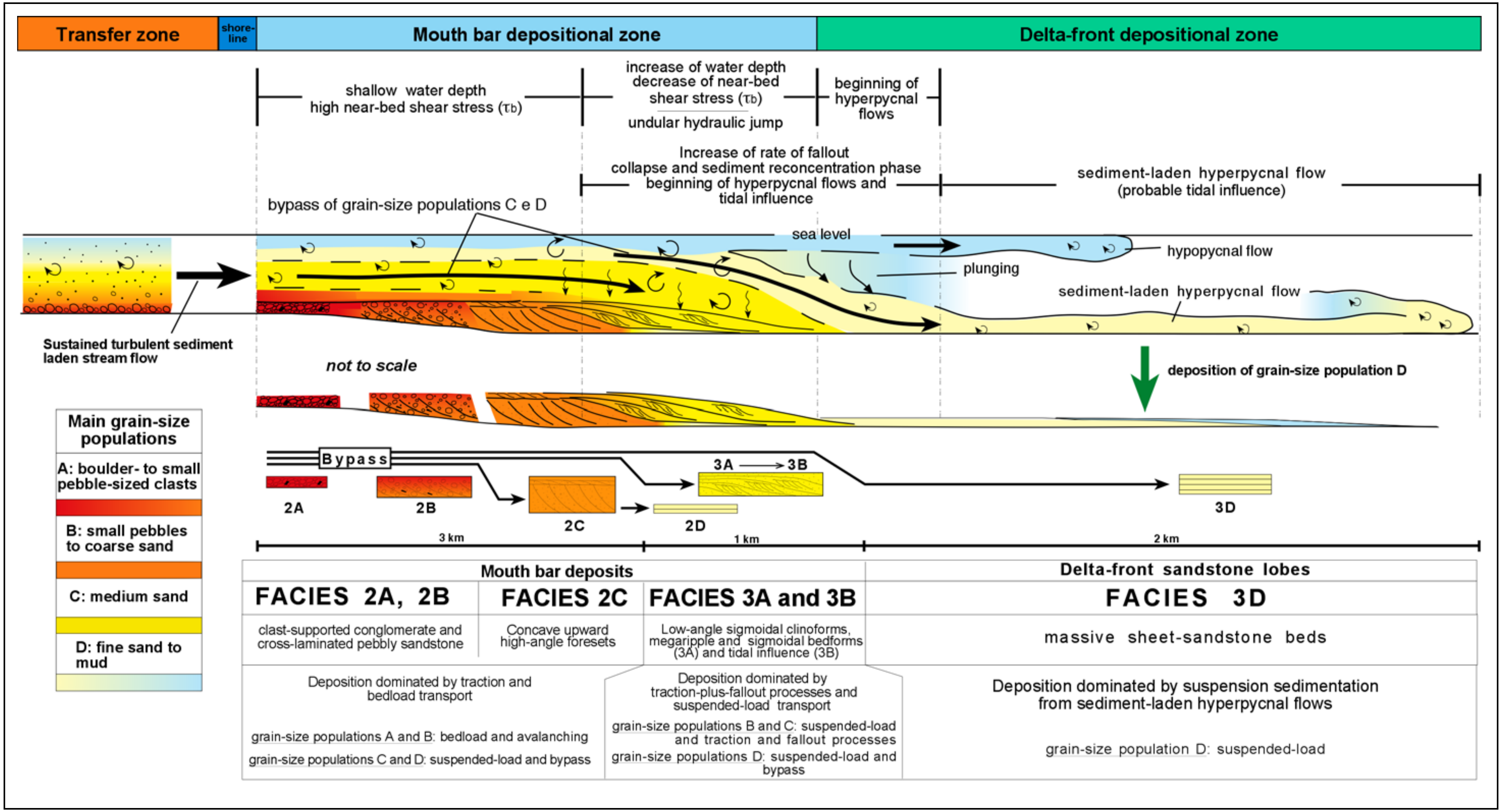

Fig. 15 - Diagram showing the type 2 facies tract deposited by a sediment-laden stream flow (SLSF) entering seawater. The main flow transformations occurring during downslope motion are also shown.

The T3 facies tract and the interaction between fluvial-floods entering seawater and tidal currents. Facies tract T2, as mentioned above, characterizes the proximal and intermediate zone of sandstone wedges R4, R5 and R6, whereas facies tract T3 characterizes only the more distal zones of the R5 and R6 units and for this reason facies tract T2 is interpreted as forming before facies tract T3 (Crumeyrolle et al. 1992). The deposition of facies tract T2, therefore, can contribute to the formation of the dynamic conditions for the generation of facies 3A through the creation of a morphologic step, which at that time, represented the delta-front slope (see also Crumeyrolle et al. 1992). In other words, the progressive forestepping of facies 2C can produce a morphologic step that separates a shallow water proximal zone from a more deeper distal zone. Therefore, if the proximal zone is characterized by the bypass of high-velocity flood-related gravity flows entering seawater exerting high-shear stresses and the sediment transport occurs mainly as bedload, the zone downcurrent to facies 2C will be characterized by a progressive flows deceleration with the consequent progressive loss of transport capacity and increasing fallout rate (Fig. 15). This zone, in which facies 3A is deposited, is characterized by the coexistence of fallout of the coarser grain-size populations (coarse and medium sand) and the bypass of the finer grain-size populations (fine sand and silt) that through a gravitational collapse, as described by McLeod et al. (1999) in a laboratory experiment, will produce a hyperpycnal flow. In this zone, moreover, where the progressive deceleration and lateral spreading of jet flow are recorded, there is also the possibility of generating a hydraulic jump (Wright & Coleman 1974) the nature of which should be undular (Allen 1982), since in facies 3A there are no significant erosional surfaces or scours that can be associated to a broken hydraulic jump (Allen 1982).

The origin of low-angle clinoforms with sigmoidal geometry could depend on various controlling factors; for example, according to the experimental works of Jopling (1965), it could be obtained by the combination of a unidirectional component and an oscillatory "wave" component. In the case of the Roda Sandstone, this could be represented by the pulsating nature of the SLSF entering seawater where the origin of the oscillatory component can be caused by various processes including a semidiurnal tidal cyclicity (Tab. 2). In this case, the cyclic wave loading of the oscillatory component tends to modify the shape of foreset slopes through the destruction of the uppermost part of the foresets producing a low angle profile. Therefore, the major effect of an oscillatory component in a pulsating SLSF entering seawater is the rounding of the relatively sharp brinkline (i.e. the zone of flow separation) shearing off the deposits of the uppermost part of the foresets. This process would yield a smooth convex up profile that, joining the lower concave part of the foreset, can develop an s-shaped or sigmoidal profile. Furthermore the convex-concave geometry can also be favoured by the variation with the distance of the near bed shear stress and so of the rate of fallout associated to the progressive deceleration of these high-velocity gravity flows entering seawater; when, in fact, the water depth increases, the near bed shear stresses decreases and sediment is allowed to deposit at the foreset region, with gradually decreasing rates towards deeper. The megaripple and sigmoidal bedforms that characterize low-angle sigmoidal clinoforms of facies 3A (Fig. 11), even if a weak tidal influence can not be completely ruled out, are here interpreted as being related to the traction and traction-plus-fallout processes that occur in this zone. These bedforms, therefore, record the fallout of the coarse and medium sand and the bypassing of fine sand and silt through the formation of hyperpycnal flows, which are responsible for the deposition of the delta-front sandstone lobes of the facies 3D (Figs 4A, 5 and 15). Specifically, these sigmoidal and megaripple bedforms of facies 3A can essentially be seen as indicators of a sediment bypass (Fig. 16A).

In particular, in the R5 unit (Figs 4, 5, 12) facies 3A passes downcurrent into facies 3D through facies 3B and 3C. The latter, on the basis of the sedimentary structures described in Tab. 3, can be interpreted as subtidal bars (Mutti et al. 1988; Nio & Yang 1991; Crumeyrolle et al. 1992). In facies 3C (Fig. 16C), the well-developed alternations of thick and thin sigmoidal bundles can, in fact, be seen as recording neap-spring cycles in a semidiurnal tidal regime in which the thin bundles with preserved mud couplets correspond to weak currents during neap-tide whereas the thicker bundles record the strong dominant currents of the spring tide. However, it is important to stress that facies 3C does not show any genetic relationship with facies 3D whereas facies 3B (Fig. 16B) passes up and downcurrent into facies 3A and 3D respectively (Figs 4A and B, 5, 12). In the R6 unit facies 3C is not present and facies 3A passes gradually downcurrent into facies 3B that, in turn, evolves into the delta-front sandstone lobes of facies 3D (Figs 4, 5, 12, 14). So if the subtidal bars of facies 3C in the R5 unit tend to rework the delta front represented by facies 3A, facies 3B in the R5 and R6 units can be interpreted as the distal part of a flood-dominated mouth bar affected by a tidal influence as indicated by the common presence of bidirectional structures directed toward south-west (Figs 12, 13C).

In the Roda Sandstone, the tidal influence present in the R5 and R6 units, is testified by facies 3B and 3C (Tab. 3). These facies characterize the transition zone between the distal part of a flood-dominated mouth bars (facies 3A) and the delta-front sandstone lobes re-

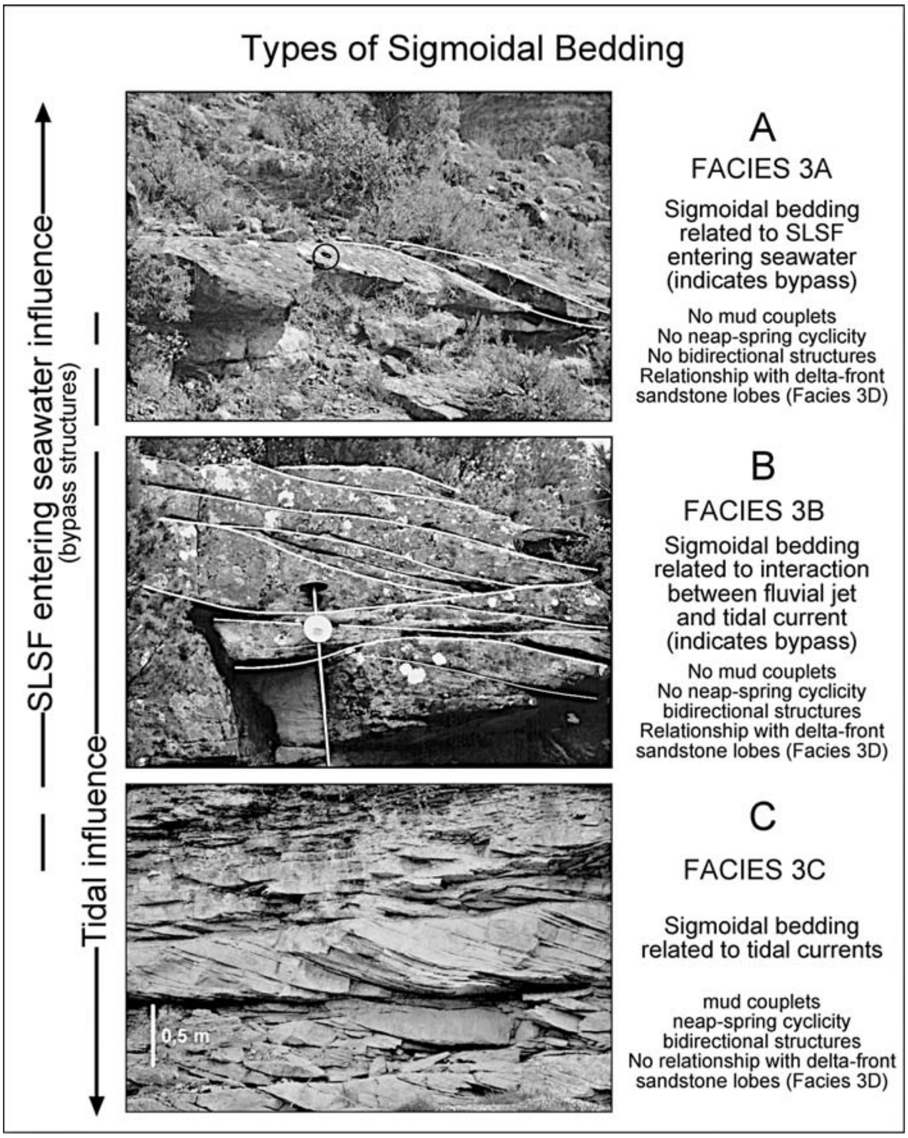

Fig. 16 - Diagram showing the three types of sigmoidal-cross stratification that characterize facies 3A, 3B and 3C respectively. A is located in the R6 unit (log 13 in Fig. 4), B in the R6 unit (log 27 in Fig. 4A) and C in the R5 unit (log 18 in Fig. 4B).

lated to these deposits (facies 3D, Figs 4, 5). In this zone (seaward of log 11, Fig. 4), therefore, there is an interaction between the processes associated with flood-related gravity flows travelling toward south-west and tidal currents oriented more or less north-south, parallel to the structural confinement created by the Roda-Turbon thrust (Figs 1C, 2). This is supported by the analysis of the paleocurrents measured within the mouth bars facies (Fig. 17). This demonstrates that from proximal flood-dominated facies (facies 1A; 1B and 2B; 2C) to more distal tidally-influenced ones (facies 3B) the paleocurrents tend to shift progressively from south-west towards north-west indicating that the jet flows of the SLSF entering seawater and related hyperpycnal flows were forced to deflect northward by tidal currents approximately directed in the same direction (cf. Wright & Coleman 1974). This deflection could also have been enhanced by the topographic high related to Roda-Turbon anticline (Fig. 17), as shown by the substantial lack of time equivalent sandstone deposits of Roda Sandstone in the Esdolomada area, i.e. the zone immediately to the west of Roda-Turbon anticline (see log H, Figs 2A, 3).

Furthermore, as shown in Tab. 3 and Fig. 16, facies 3A, 3B and 3C are characterized by three different types of sigmoidal bedform that are considered to represent the result of this interaction. In other words, even if the sigmoidal-cross stratification is a sedimentary structure whose understanding, more likely, needs further field and experimental work, it is here suggested that three different types of sigmoidal bedforms can exist in association with three different types of flows. Explicitly, since sigmoidal bedforms associated to flood-related gravity flows entering seawater (facies 3A, Fig. 16A), and to tidal currents (facies 3C, Fig. 16C) have been observed, it is here considered that there also exists the possibility that sigmoidal bedforms can result from a combination between SLSFs entering seawater and tidal currents. This processes interaction is thought to be recorded in the Roda Sandstone mainly by facies 3B (Fig. 16B).

The sigmoidal cross-stratification can be seen, like the HCS, as a multigenetic and ubiquitous sedimentary structure since there are numerous environments in which it can be recognized and a variety of processes that can produce it. Sigmoidal bedforms, for example, can be found not only in mouth bars and in tidal deposits but also in fluvial deposits (Røe 1987; Mutti et al. 1996). From a hydrodynamic point of view, on the contrary, even if, traction and traction-plus-fallout processes related to unidirectional flows both with high and low fallout rates at the dune-plane bed transition can deposit sigmoidal bedforms (Saunderson & Lockett 1983; Røe 1987), it is reasonable to propose that this type of structure can also be deposited by tractive processes related to a pulsating combined flow characterized by an oscillatory component that is not necessarily always related to a tidal cyclicity (Tinterri 1997, 2006b). As indicated in Tab. 2, an oscillatory component in a SLSF entering seawater and related hyperpycnal flows can be generated in different ways. Therefore it is the author's opinion that there should also exist a relationship between sigmoidal bedforms and HCS; i.e. a continuum, both in terms of types of flow and types of sedimentary structure, between coarse-grained sigmoidal bedforms deposited in the mouth bar by traction processes related to pulsating SLSF entering seawater and fine-grained HCS in delta-front sandstone lobes generated by traction plus fallout processes related to sediment-laden hyperpycnal flows characterized by symmetric or slightly asymmetric oscillatory combined flows (Tinterri 1997, 2006b).

Similarly, the massive tabular sandstone beds of facies 3D that are interpreted as delta-front sandstone lobes deposited by sand-laden hyperpycnal flow (Tinterri 1999a) could also be associated to this type of interaction. Even if the delta-front sandstone lobes are generally graded beds characterized by HCS, in the R5 and R6 units, they are essentially massive (Fig. 13D). The origin of a massive bed is usually related to a sudden deceleration of a sediment-laden gravity flow that, through a gravitational collapse (McLeod et al. 1999), can produce fallout rates sufficiently high to suppress tractive processes. In the case of the Roda Sandstone, this phenomenon could be enhanced not only by the

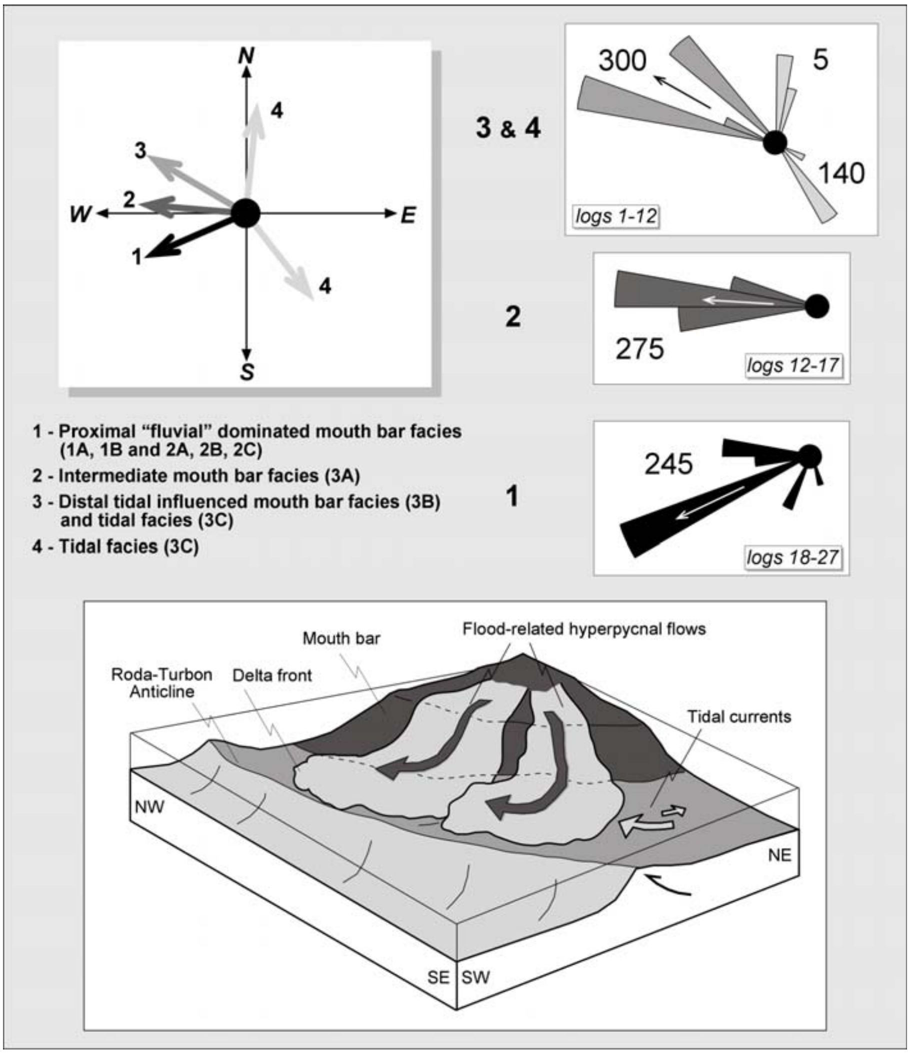

Fig. 17 - Paleocurrents of type 1 and type 2 deposits in which the change of direction from proximal to distal zones can be noted. Below a schematic diagram reproduces the paleogeography of the Roda Basin and the behaviour of the flood-related hyperpycnal flows due to the interaction with tidal currents and topographic confinement represented by Roda-Turbon anticline.

relatively shallow water seaward of the river mouth but also, more probably, by the friction associated both to flood and ebb tidal currents and also by the tectonic confinement related to the north-west/south-east oriented Roda-Turbon high that tends to decelerate the hyperpycnal flow evolving toward west (see Figs 15, 17).

In conclusion, type 2 deposits can be interpreted as tidally influenced mouth bars and related delta-front sandstone lobes deposited by SLSFs entering seawater in a flood-dominated river-delta system.

Topographic control on deposition

On the basis of the concept introduced in previous sections, the Roda basin is a topographically controlled basin in which the Roda Sandstone deposition was influenced by a series of synsedimentary folds oriented roughly northwest-southeast (Fig. 2; Lopez-Blanco et al. 2003) and by a structural confinement represented by the Roda fold related to the Roda-Turbon thrust (Figs 1C, 2, 17). The topographic confinement, as mentioned above, would have controlled not only the enhancement and the direction of tidal currents but also the eventual phenomena of reflection and deflection that the flood-related hyperpycnal flows could have undergone against the topographic highs. In particular, since the Roda folds should produce soft topographic highs and lows, it is plausible that these morphologic obstacles tended to produce progressive decelerations and deflections rather than sudden impacts and reflections.

As can be observed in the stratigraphic-cross section of Fig. 4, overall changes in thickness seem to coincide with some of the main folds described by Lopez-Blanco et al. (2003) (see also Fig. 2B). In particular, the Canerol anticline would explain very well the anomalous thickness of highly-bioturbated fine-grained massive sandstone at the base of the R4 unit in a depocenter or syncline located in the north of the Canerol creek (zone between logs 4 and 8 in Figs 4A and 2B). These deposits can, in fact, be interpreted as delta-front sandstone lobes (facies 2D) related to facies 2C derived from the progressive deceleration of the sand-laden hyperpycnal flow against the Canerol anticline. Moreover, coinciding with this anticline, the carbonate strata of the R4 unit (Fig. 4), that represent the maximum flooding surface at the top of the R4 unit, show an abrupt increase in thickness signaling shallower water. In the same way, the high related to the Roda anticline could explain not only the massive delta-front sandstone lobe of facies 3D in the R5 and R6 units (see above, Fig. 4A) but also the progressive deviation of the paleocurrents toward north-west.

Sequence stratigraphy interpretation of the Roda Sandstone

The Roda Sandstone, as shown in Fig. 4, is made up of six depositional sequences of different hierarchical order, ranging in thickness from 10 to about 100 metres (see Fig. 18), each of which is characterized by a basal deltaic sandstone wedge (R1, R2, R3, R4, R5, R6) that passes upward into a siltstone and mudstone interval. In particular, the transgressive systems tract located directly above the R6 unit is indicated as the R7 unit (Fig. 4). The depositional sequences, containing the basal sandstone units R1, R2, R3, are approximately ten metres thick and can be considered elementary depositional sequences (i.e. EDS, according to Mutti et al. 1994). The EDSs, in fact, represent the highest frequency cyclicity of sequence stratigraphic significance recognizable in the sedimentary succession and they can stack vertically to form stratigraphic units of higher hierarchical order such as small-scale and large scale composite depositional sequences and allogroups (see Mutti et al. 1994 for more details). The other relatively larger volume depositional sequences, ranging in thickness from 50 to about 100 metres, are characterized by the R4, R5, R6 units and may be interpreted as small scale composite depositional sequences since they are composed of more EDSs. In EDSs of the Roda Sandstone, the upper boundary of the basal sandstone units is sharp and often characterized by mixed and carbonate sediments due to the benthic fauna organism colonization that can occur when the fluvial sediment supply is interrupted (Fonnesu 1984; Molenaar & Martinius 1996; Calabrese 1999). Thus, these layers can also be interpreted as representing small condensed surfaces and hard grounds indicating an abrupt reduction of sediment supply due to the deactivation of fluvial systems. In particular the R1 unit pass laterally into a tabular bioclastic bed (storm bed of Crumeyrolle et al. 1992) that represents a key bed for all over Roda zone (Figs 2, 4). Regional stratigraphic studies (Mutti et al. 1988, 1994), however, permit to advance the hypothesis that this bed could be time-equivalent with the tsunami bed described by Mutti et al. (1985) at the base of FG1 in Ager syncline (Fig. 1A and B).

The stacking pattern analysis of these six depositional sequences of different hierarchical order reveals that they are characterized by a progressive forestepping trend culminating in the R6 unit and a backstepping recorded by the uppermost R7 unit. In particular the R6 unit is characterized by an abrupt regression of the depositional zone (Fig. 4) recorded also by an erosive basal surface (the red line in Figs. 4, 12, see also Fig. 11A) that truncates the underlying deposits of the R5 unit. According to Mutti et al. (1996), this erosive surface is associated to a tectonic uplift producing the re-

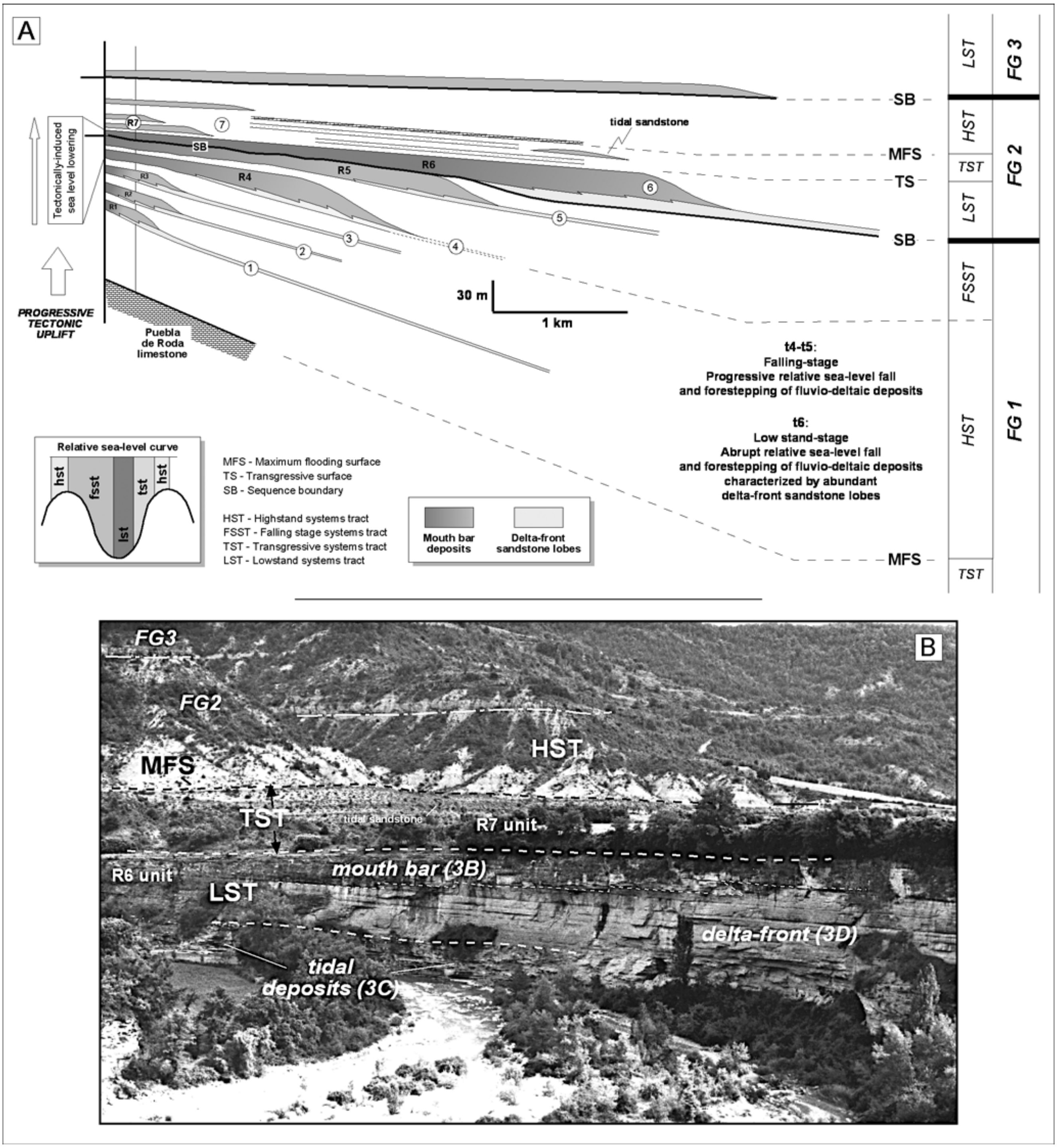

Fig. 18 - A) Diagram showing the sequence stratigraphy interpretation of the Roda Sandstone. B) Overview of the FG2 depositional sequence made up of the basal fluvio-deltaic deposits of the R6 unit (lowstand systems tract, LST) overlain by transgressive facies (TST, R7 unit) (see logs 18 and 19 in Fig. 4B). The latter is sharply bounded by a maximum flooding surface (MFS) that marks the passage into highstand mudstone (HST), (see also Mutti et al. 1988, their plate IIA). The passage to the FG3 depositional sequence is also indicated.

newal and rapid downward shift of relatively coarse-grained sediment (Fig. 18). Consequently, the basal fluvio-deltaic sandstone that characterizes the depositional sequences are here interpreted to derive from flood-dominated gravity flows produced in response to a climate change after periods of tectonic uplift of adjacent orogenic wedges (Fig. 18).

Although the Roda Sandstone has been interpreted as a low-stand systems tract of FG2 (Mutti et al. 1988; Crumeyrolle et al. 1992), the presence of this erosive surface, togheter with the progressive forestepping trend, is here considered of primary importance because it can be interpreted as a sequence boundary. Consequently this erosive surface may be seen also as the sequence boundary between FG1 and FG2 that was previously placed at the base of the Roda Sandstone (see Fig. 3), making it possible to subdivide the stratigraphic succession of the Roda Sandstone into two parts: 1) an overlying depositional sequence, approximately one hundred metres thick, characterized by the R6 unit that represents the LST of FG2, consisting of a low-stand deltaic wedge formed by tidal-influenced mouth bars and by a large volume of delta-front sandstone lobes, and 2) an underlying part, constituted by the high frequency depositional sequences characterized by the R1, R2, R3, R4 and R5 basal sandstone units. On the basis, among other things, of the considerations on the Figols Group previously introduced in the general stratigraphic framework paragraph (see above), this basal part of the Roda Sandstones (R1 to R5) can be interpreted as the highstand of FG1 where, however, the sea level was probably already falling, as testified by the roughly offlap geometry and by the general progressive increase of sediment input and amount of basinward shifts of the fluvio-deltaic depositional zone. These observations make it possible to advance the hypothesis that at least a part of the lower portion of the Roda Sandstone (from R1 to R5) could record a falling stage systems tract (FSST) defined, according to Plint & Nummedal (2000) as a stratigraphic unit produced during a phase of relative sea-level fall and that lies above a HST and below a LST characterized by a stacking pattern composed of forestepping high-frequency sequences with offlap geometry. The recognition of this type of geometry in outcrop is, however, very difficult. Nevertheless the beginning of the FSST in the Roda Sandstone could be tentatively located at the base of the R4 high-frequency depositional sequence because of the abrupt increase in the volume of sediment input (Figs 4A, B and 18). Therefore, the depositional sequences from R4 to R5 can be interpreted as a response to a longer-term sea-level fall (Fig. 18) punctuated by smaller-scale relative sealevel fluctuations controlled by a progressive tectonic uplift and subsidence, that could justify the small scale condensed surface of R4 unit.

Finally, the R6 unit is capped by transgressive deposits (the R7 Unit) characterized in the proximal zone by small volume mouth bars of upward decreasing volume that pass basinward into highly bioturbated and fossiliferous very fine sandstone and siltstone in which tidal sandstones constituted by sigmoidal bedforms with paleocurrent directed toward the north can be recognized (Figs 4B, 18). Through a sharp contact, marking the maximum flooding surface, these transgressive deposits are then covered by highstand mudstones (Fig. 18A, B). The base of FG 3 is marked by the first arrival of coarse-grained mouth bars (Figs 3, 18; see also Mutti et al. 1988).

The transgressive systems tract, the maximum flooding of the R7 unit and the lower boundary of the FG3 depositional sequence have also been recently documented by Torricelli et al. (2006) in Merli-Esdolomada zone (log I of Fig. 3) on the basis of the environmental meanings of dinoflagellates cyst, palynofacies and foraminiferal records (see also Gaboardi 1996). In particular, the maximum flooding interval is characterized by a rich and diverse microfauna, highest relative abundance of marine phytoplankton and typical neritic dynoflagellate cyst (dinocyst) assemblages dominated by *Spiniferites* and *Cordosphaeridium*. On the contrary, the final phase of the highstand system tract, in proximity of the FG3 sequence boundary, is characterized by a decrease in abundance and diversity of dinocysts, with the dominance of the lagoonal genus *Polyspharidium* and by decreased microfaunal diversity (discorbids, miliolids and larger foraminifers). This mass introduction of lagoonal indicators into more open marine environments is interpreted to be the expression of a sudden relative sea level fall, with a consequent increase of sediment flux to the sea and a basinward shift of the optimum habitats of marginal marine species (Torricelli et al. 2006; see also Dominici and Kowalke 2007).

In conclusion, the erosive sequence boundary within the Roda Sandstone (red line in Fig. 4) may also represent the sequence boundary between FG1 and FG2 that was previously placed (Mutti et al. 1988; Crumeyrolle et al. 1992) at the base of the Roda Sandstone (see Fig. 3). Consequently, the FG2 depositional sequence, that is approximately 100 m thick, results as being composed of a LST represented by the R6 unit and a TST represented by the R7 unit that passes upward into highstand mudstone as shown in Fig. 18.

Summary and Conclusions

• Sedimentology

It is here considered that a first important detailed stratigraphic model of the Roda Sandstone was provided by Crumeyrolle et al. (1992; their attachment 1) (see also Crumeyrolle, 2003). The main innovation of this paper in respect to Crumeyrolle et al. (1992) is the facies interpretation influenced by the discovery of well developed delta-front sandstone lobes, not only in proximal and intermediate zones (T1 and T2 facies tract) but also in more distal zones, seaward of log 11 of figure 4A (T3 facies tract). Therefore this work, for the first time, highlights well distinctive mouth bars and lobe elements in the Roda Sandstone thanks to a new high resolution stratigraphic framework represented by figure 4A.

The detailed facies analysis of the sandstone wedges (R1-6) that characterise the Roda Sandstone, in fact, has shown that the R1, R2 and R3 units are characterized by relatively small-volume mouth bars passing downcurrent into attached massive and highly fossiliferous delta-front sandstone lobes of facies 1Cd (T1 facies tract, Figs 5, 7A), whereas the relatively larger volume R5 and R6 units are characterized by three growing stages each of which is characterized by a well determined type of facies sequence and respective facies tract (Figs 5, 7A, B, C). In these units, in fact, it is possible to observe the passage from proximal mouth bars and delta-front sandstone lobes with HCS (the T1 facies tract) to distal tidally-influenced mouth bars and related massive sandstone lobes (the T3 facies tract) through intermediate mouth bars that can pass downcurrent into massive bioturbated sandstone lobes (the T2 facies tract), (Figs 5A, B). The R4 unit, on the contrary, can be seen as a sandstone wedge with intermediate characteristics between the lower and upper units because in this unit T3 deposits are absent and thus it is composed by only two growing stages represented by T1 and T2 deposits. The facies tracts characterizing these deposits are interpreted as being related to various types of sediment-laden stream flows (SLSFs) entering seawater produced in a flood-dominated river-delta system. In particular, facies tract T1 is interpreted as deposited by coarse-grained composite sediment-laden stream flows (CSLSFs), the T3 facies tract by turbulent SLSF whereas the T2 facies tract that has intermediate facies characteristics (facies 2A, Tab. 3 and Fig. 5) may be interpreted as deposited both by composite and turbulent SLSFs (Fig. 15). In this way, if the gravity flows that produced facies tract T1 were characterized by coarse grained dense inertial parts, the successive SLSFs that produce facies tracts T2 and T3, became progressively dominated by turbulence and by a vertical stratification of grain sizes (Fig. 5).

The nature and origin of these types of gravity flows may depend upon: 1) the drainage-basin conditions related to the ratio between the rate of tectonic uplift which determines the morphometric properties of the catchment, and the rate of climatic change, which mainly controls the amount of rainfall and consequently the surface runoff and 2) the nature of catchment bedrocks. These variables control the type of gravity flow and its efficiency. In general, the drainage basins that tend to favour the generation of dense inertial flows are very small and experience a rate of uplift higher than the rate of incision of the fluvial processes that produce high-gradient longitudinal profiles (Hovius 1998; Mutti et al. 1996). On the contrary, the drainage basins that tend to favour the generation of SLSFs are characterized by larger basins and rates of fluvial incision higher than the tectonic uplift rates. This phenomenon produces a concave upward longitudinal profile with a high-gradient drainage zone and low-gradient transfer zone (Hovius 1998; Mutti et al. 1996). All things being equal, moreover, the type of gravity flow can also depend on the type of the bedrock found in the drainage basin (Blair 1999; Moscariello et al. 2002). For example, as in the case of the Roda Sandstone (see general geologic setting section), catchment bedrocks characterized by massive crystalline rocks such as granites and granodiorites tend to yield weathering mantle constituted only by coarse grain size populations (medium/coarse sand to boulders) without the fines (silt and clay). This tends to prevent the generation of debris flows and to favour the generation of turbulent flood flows such as SLSFs in which the transport occurs mainly as bedload and suspended load.

• Interaction between flood-related gravity flows and tidal currents

The Roda Sandstone is a system of mouth bars and delta-front sandstone lobes deposited in a flood-dominated river-delta system in which the deposition was strongly controlled by an interaction between flood-dominated gravity flows entering seawater, tidal currents and topographic confinement. The structural high represented by the Roda-Turbon fold, in fact, not only enhanced the tidal currents but also acted as a topographic threshold for the hyperpycnal flows as suggested by the lack of the time-equivalent sandstone deposits of the Roda Sandstone in Esdolomada H log (Figs 2, 3). Also, the analysis of the paleocurrents show that, moving progressively downcurrent, the fluvial input that was directed towards south-west in the proximal zone (facies tract T1 and facies 2B, 2C), tended progressively to turn toward west (facies 3A) and then toward north-west in more distal zones (facies 3B). This change is here considered related to the interaction between the structural confinement due to the Roda-Turbon fold and tidal currents that had a north-west/south-east direction (Fig. 17).

This interaction is evident especially in the more distal facies tract T3 in which facies 3A, characterized by sigmoidal and megaripple bedforms related to deltaic jet flows, passes downcurrent into massive delta-front sandstone lobes (facies 3D) through intermediate facies 3B and 3C. The latter are characterized by clear tidal sigmoidal bedforms in the R5 unit (facies 3C) and by tidally-influenced flood-dominated deposits in the R5 and R6 units (facies 3B). In a situation of this type, the hypothesis is here advanced that three type of sigmoidal bedforms can exist: 1) those associated with flood-related gravity flows entering seawater (facies 3A, Fig. 16A), 2) those related to tidal currents (facies 3C, Fig. 16C), and 3) those related to the combination between SLSFs entering seawater and tidal currents (facies 3B, Fig. 16B). In other words, it is here considered that a large part of the sigmoidal bedforms of facies 3A and 3B could be interpreted as being related to traction and traction-plus-fallout processes associated with pulsating combined flows generated by the interference between a flood-related gravity flow entering seawater and an oscillatory component (Tab. 2) in which, especially for facies 3B, also the semidiurnal ciclicity of a tidal current could have had an important role . The sigmoidal bedforms, in fact, can be considered ubiquitous, multigenetic sedimentary structures and it is here suggested that their more correct interpretation can derive especially by a careful analysis of facies sequences (Fig. 7) and stratigraphic framework in which sigmoidal bedforms are found (Figs 4 and 5). Using this approach, the sigmoidal bedforms of facies 3A and 3B have been interpreted as sedimentary structures indicating the bypass (Fig. 15) of finer grain-size populations (fine sand to mud) that, through a gravity transformation related to the deceleration of flood gravity flows entering seawater, can collapse to form sediment-laden hyperpycnal flows responsible for the deposition of the delta-front sandstone lobes of facies 3D.

• Stratigraphy

The Roda Sandstone is made up of six depositional sequences of different hierarchical order, ranging in thickness from 10 to about 100 metres, each of which is characterized by a basal sandstone unit (R1-6) that passes upward into a siltstone and mudstone interval. These units record a progressive forestepping culminating in the depositional sequence characterized by the R6 sandstone unit that represents the approximately 100 m thick FG2 depositional sequence (Fig. 18). The abrupt regression of the R6 unit is characterized by a basal erosive surface truncating the underlying mouth bars of the R5 unit (Fig. 11) that is here interpreted as a sequence boundary (red line of Fig. 4). This erosive surface, therefore, makes it possible to divide the Roda Sandstone, whose sedimentary succession has always been interpreted as the lowstand delta of the FG2, into two parts: 1) an underlying highstand systems tract (HST) and falling-stage systems tract (FSST) of the FG1 (units R1 to R5) and 2) the overlying FG2 depositional sequence characterized by a low-stand delta (the R6 unit) that passes upward into highstand mudstone through a transgressive systems tract represented by the R7 unit (Fig. 18).

Acknowledgements: The author is deeply gratelful to Emiliano Mutti for his helpful review and for his plentiful advice and to Marco Roveri for his constructive suggestions. Stefano Angella and Maria Sgovetti are thanked for the helpful discussions in the field and about the aerial photographs respectively. Reviews by Franco Fonnesu, Philippe Crumeyrolle, and the Editor Maurizio Gaetani significantly improved the manuscript. Many thanks also go to Jesse Melick and Paul Sears for their help in the final phase of editing. Much of this research was funded by the Consiglio Nazionale delle Ricerche, Rome, and by MURST (Coordinator, Emiliano Mutti).

REFERENCES

Allen J.R.L. (1982) - Sedimentary structures: Their Character and Physical Basis. Developments in Sedimentology (volume I), V. of 593 pp., Elsevier Libr., Amsterdam.

Angella S. (1999) - Analisi stratigrafico-sedimentologica del Gruppo di Figols all'interno dei bacini di Ager e Tremp (Pirenei centro meridionali). Ph.D. Thesis, University of Parma, V. of 108 pp., Parma.

Barberà X., Marzo M., Reguant S., Samsò J.M., Serra-Kiel J. & Tosquella J. (1997) - Estratigrafia del Grupo de Figols (Paleogeno, Cuenca de Graus-Tremp, NE de España). *Rev. Soc. Geol. España*, 10: 67-84, Madrid.

Best J.L. (1992) - Sedimentology and event timing of a catastrophic volcanoclastic mass flow, volcano Hudson, Southern Chile. *Bull. Volcanology*, 54: 299-318, Berlin Heidelberg.

Blair T.C. (1999) - Cause of dominance by sheetflood vs. debris flow processes on two adjoing alluvial fans, Death valley, California. *Sedimentology*, 46: 1015-1028, Oxford.

Boersma J.R. & Terwindt J.H.J. (1981) - Neap-Spring tide sequences of intertidal shoal deposits in a mesotidal estuary. *Sedimentology*, 28: 151-170, Oxford.

Calabrese L. (1999) - Stratigrafia fisica e analisi di facies del Gruppo di Figols (Eocene, Pirenei centro meridionali). Studio delle relazioni tra sistemi carbonatici e silico-clastici. Ph.D. Thesis, University of Parma, V. of 134 pp., Parma.

Campbell C.V. (1967) - Lamina, laminaset, bed and bedset. *Sedimentology*, 8: 7-26, Oxford.

Carminatti M. (1992) - Stratigrafia fisica e modellizzazione sismica inversa del Gruppo di Figols affiorante tra la Val Isabena e la Val Esera (Eocene inferiore, Pirenei centro-meridionali, Spagna). Ph.D. Thesis, University of Parma, V. of 164 pp., Parma.

Carminatti M. & Villa G. (1993) - High resolution stratigraphy of the Ilerdian Figols Allogroup (South Pyrenees, Spain). *AAPG Annual Convention New Orleans*, Abstract volume: 83, Tulsa.

Crumeyrolle Ph. (2003) - Stratal architecture and facies assemblages of the Roda Sandstone lowstand wedge (south-central Pyrenees). *AAPG International Conference and Exhibition*, Barcelona, Spain, 21-24 september 2003, Geological field Trip 4 (Part II), 51 pp., Tulsa.

Crumeyrolle Ph., Lesueur J.L., Claude D. & Joseph Ph. (1992) - Architecture et faciés d'un prisme deltaique de bas niveau marin: les grés de Roda (bassin eocéne sud Pyrénéen). Livret-guide de l'excursion ASF, 25-27 September 1992, 36 pp., Paris.

Dewey J.F., Helman M.L., Turco E., Hutton D.H.W. & Knott S.D. (1989) - Kinematics of the western Mediterranean. In: Coward M.P., Dietrich D. & Park R.G. (Eds) - Alpine tectonics, *Spec. Publ. Geol. Soc. London* 45: 265-283, London.

Dominici S. & Kowalke T. (2007) - Depositional dynamics and the record of ecosystem stability: early Eocene coastal communities in the pyrenean foreland, Spain. *Palaios*, 22: 268-284, Tulsa.

Edwards D.A., Leeder M.R., Best J.L. & Pantin H.M. (1994) - On experimental reflected density currents and the interpretation of certain turbidites. *Sedimentology*, 41: 437-461, Oxford.

Eichenseer H. (2003) - Stratigraphic styles influenced by thrust tectonics, architecture and facies of lowstand deltaic wedges and transgressive to highstand carbonate banks (upper Paleocene to lower Eocene, central southern Pyrenees). *AAPG International Conference and Exhibition*, Barcellona, Spain 21-24 september 2003, Geological field Trip 4 (Part I), 77 pp., Tulsa.

Eichenseer H. & Luterbacher H.P. (1992) - The marine paleogene of the Tremp Basin (NE Spain) – depositional sequences, facies history, biostratigraphy and controlling factors. *Facies*, 27: 119-152, Erlangen.

Fonnesu F. (1984) - Estratigrafia fisica y analisis de facies de la sequencia de Figols entre al Rio Noguera Pallaresa e Iscles (prov. de Lerida y Huesca). Ph.D. Thesis, Universidad Autonoma de Barcelona, V. of 317 pp., Barcelona.

Gaboardi S. (1996) - Relationship between foraminiferal assemblages and depositional sequences in the Merlì Est section (Figols Allogroup – south-central Pyrenees – Lower Eocene). *Riv. It. Paleont. Stratigr.*, 102: 237-266, Milano.

Garrido Megias A. (1973) - Estudio geologico y relacion entre tectonica y sedimentacion del Secundario y Terciario de la vertiente meridional pirenaica en su zona central (Provincias de Huesca y Lerida). Ph.D. Thesis, University of Granada, V. of 395 pp., Granada.

Hovius N. (1998) - Control on sediment supply by large rivers. In: Shanley K.W. & McCabe P.J. (Ed.) - Relative Role of Eustasy, Climate, and Tectonism in Continental Rocks, *SEPM Spec. Publ.* 59: 3-16, Tulsa.

Jopling A.V. (1965) - Hydraulic factors controlling the shape of laminae in laboratory deltas. *J. Sed. Petr.*, 35: 777-791, Boulder.

Leithold E.L. & Bourgeois J. (1984) - Characteristics of coarse-grained sequences deposited in nearshore, wave-dominated environments-examples from the Miocene of south-west Oregon. *Sedimentology*, 31: 749-775, Oxford.

Kneller B. (1995) - Beyond the turbidite paradigm: physical models for deposition and their implications for reservoir prediction. In: Hartlet A.J. & Prosser D.J. (Eds) - Characterization of Deep Marine Clastic Systems, *Geol. Soc. Spec. Publ.* 94: 31-49, London.

Lopez-Blanco M. & Marzo M. (1998) - The Roda sandstone: transgressive-regressive architecture of syntectonic, tidal-influenced deltaic sand wedges. *15th IAS Congress*, Alicante (Sp), Field Trip Guidebook, 224-230, Alicante.

Lopez-Blanco M., Marzo M. & Muñoz J.A. (2003) - Low amplitude, synsedimentary folding of a deltaic complex: Roda Sandstone (lower Eocene), south-pyrenean foreland basin. *Basin Research*, 15: 73-95, Oxford.

Luterbacher H.P. (1969) - Remarques sur la position stratigraphique de la Formation d'Ager (Pyrenees meridionales). *Mem. Bur. Rech. Geol. Min.*, 69/III: 225-231, Paris.

Martini P.I., Baker V.R. & Garzon G. (2002) - Flood and megaflood processes and products: recent and ancient examples. *IAS Spec. Publ. 32*, Blackwell Science, 312 pp., Oxford.

McLeod P., Carey S. & Sparks S.J. (1999) - Behaviour of particle-laden flows into the ocean: experimental simulation and geological implications. *Sedimentology*, 46: 523-536, Oxford.

Mey P.H.W., Nagtegaal P.J.C., Roberti K.J. & Hartevelt J.J.A. (1968) Lithostratigraphic subdivision of post-hercynian deposits in the south-central Pyrenees, Spain. *Leidse Geologische Mededelingen*, 41: 221-228, Leiden.

Milliman J.D. & Syvitski J.P.M. (1992) - Geomorphic/Tectonic control of sediment discharges to the ocean: the importance of small mountains rivers. *J. Geol.*, 100, 525-544, Chicago.

Molenaar N. & Martinius A.W. (1996) - Fossiliferous intervals and sequence boundaries in shallow marine, fan-deltaic deposits (Early Eocene, southern Pyrenees, Spain). *Paleogeogr., Paleoclim., Paleoecol.*, 121: 147-168, Amsterdam.

Molenaar N., Van de Bilt G.P., Van den Hoek Ostende E.R. & Nio S.D. (1988) - Early diagenetic alteration of shallow-marine mixed sandstones: an example from lower Eocene Roda Sandstone Member, Tremp-Graus Basin, Spain. *Sed. Geol.*, 55: 295-318, Amsterdam.

Moscariello A., Marchi L., Maraga F. & Mortara G. (2002) - Alluvial fans in the Italian Alps: sedimentary facies and processes. In: Martini P., Baker V. R. & Garzon, G. (Eds) – Flood and Megaflood Processes and Deposits – Recent and Ancient Examples, *IAS Spec. Publ. 32*, Blackwell Science, 141-166, Oxford.

Muñoz J.A. (1992) - Evolution of continental collision belt: ECORS-Pyrenees crustal balanced cross-section. In: K.R. McClay (Ed.) - Thrust Tectonics, Chapman and Hall Libr., 235-246, London.

Mulder T. & Syvitski J.P.M. (1995) - Turbidity currents generated at river mounths during exceptional discharges to the world oceans. *J. Geol.*, 103: 285-299, Chicago.

Mulder T., Syvitski J.P.M., Migeon S., Faugeres J.C. & Savoye, B. (2003) - Marine hyperpycnal flows: initiation, behaviour and related deposits. A review. *Marine and Petroleum Geology*, 20: 861-882, Amsterdam.

Mulder T., Syvitski J.P.M. & Skene K.I. (1998) - Modeling of erosion and deposition of turbidity currents generated at river mouths. *J. Sed. Res.*, 68: 124-137, Boulder.

Mutti E. (1992) - Turbidite Sandstones. ENI Agip-Istituto di Geologia, Università di Parma, V. of 275 pp., San Donato Milanese.

Mutti E., Allen G.P. & Rosell J. (1984) - Sigmoidal-cross stratification and sigmoidal bars: depositional features diagnostic of tidal sandstones. *5th IAS European Regional Meeting*, Abstract volume, 312-313, Marsiglia.

Mutti E., Davoli G., Mora S. & Sgavetti M. (1994) - The Eastern sector of the South-Central Folded Pyrenean Foreland: Criteria for Stratigraphic Analysis and Excursion Notes. Second high-resolution sequence stratigraphy conference, June 20-27 1994, V. of 83 pp., Tremp.

Mutti E., Davoli G, Tinterri R. & Zavala C. (1996) - The importance of fluvio-deltaic systems dominated by catastrophic flooding in tectonically active basins. *Mem. Scien. Geol.*, 48: 233-291, Padova.

Mutti E., Rosell J., Allen G.P, Fonnesu F. & Sgavetti M. (1985) - The Eocene Baronia tide dominated delta-shelf system in the Ager Basin. In: Mila M. & Rosell J. (Eds) - *6th IAS European Regional Meeting*, Field Trip Guide Book, 579-600, Lerida.

Mutti E., Seguret M. & Sgavetti M. (1988) - Sedimentation and Deformation in the Tertiary Sequences of the Southern Pyrenees. *AAPG Mediterranean Basin Conference, Spec. Publ. Institute of Geology, University of Parma*, Field Trip 7, V. of 153 pp., Parma.

Mutti E., Tinterri R., Benevelli G., di Biase D. & Cavanna G. (2003) - Deltaic, mixed and turbidite sedimentation of ancient foreland basins. *Marine & Petroleum Geology*, 20: 733-755, Amsterdam.

Mutti E., Tinterri R., Di Biase D., Fava L., Mavilla N., Angella S. & Calabrese L. (2000) - Delta-front facies associations of ancient flood-dominated fluvio-deltaic systems. *Rev. Soc. Geológica España*, 13: 165-190, Madrid.

Mutti E., Tinterri R., Remacha E., Mavilla N., Angella S. & Fava L. (1999) - An introduction to the analysis of ancient turbidite basins from an outcrop perspective. *AAPG Continuing Education Course Note Series*, n. 39, V. of 47 pp., Tulsa.

Myrow P.M., Fischer W. & Goodge J.W. (2002) - Wave-modified turbidites: Combined flow shoreline and shelf deposits, Cambrian, Antartica. *J. Sed. Res.*, 72: 641-656, Boulder.

Nijman W. & Nio S.D. (1975) - The Eocene Montañana Delta (Tremp-Graus Basin, provinces of Lerida and Huesca, Southern Pyrenees, Spain). In: Rosell J. & Puigdefàbregas C. (Eds) – The Sedimentary Evolution of the Paleogene South-Pyrenean Basin, *IX Int. Cong. IAS*, part B, 1-20, Nice.

Nemec W. (1995) - The dynamics of deltaic suspension plumes. In: M.N. Oti & G.Postma (Eds) - Geology of Deltas, A.A. Balkema, Brookfield, 31-93 Rotterdam.

Nio S.D. (1976) - Marine transgressions as a factor of formation of sand waves complexes. *Geol. Mijnb.*, 55: 18-40.

Nio S.D., Siegenthaler C. & Yang C. (1984) - Facies pattern and development of the Lower Eocene Roda Sandstone, Isabena Valley, southren Pyrenees, Spain. *5th IAS European Regional Meeting*, Abstract volume, 328-329, Marsiglia.

Nio S.D. & Yang C.S. (1991) - Sea-level fluctuations and the geometric variability of the tide-dominated sandbodies. *Sed. Geol.*, 70: 161-193, Amsterdam.

Plint A.G. & Nummedal D. (2000) - The falling stage system tract: recognition and importance in sequence stratigraphic analysis. In: D. Hunt & R.L. Gawthorpe (Eds) - Sedimentary responses to forced regressions, *Spec. Publ. Geol. Soc. London*, 172: 1-17, London.

Puigdefàbregas C. (1975) - La sedimentation molasica en la cuenca de Jaca. *Pirineos*, 104: 1-188, Jaca.

Puigdefàbregas C., Muñoz J.A. & Vergés J. (1992) - Thrusting and foreland basin evolution in the Southern Pyrenees. In: K.R. McClay (Ed.) - Thrust Tectonics, Chapman and Hall Libr., 247-254, London.

Puigdefàbregas C., Samso J.M., Serra-Kiel J. & Tosquella J. (1985) - Facies analysis and faunal assemblages of the Roda sandstone Formation, Eocene of the southern Pyrenees. *VI IAS European Regional Meeting*, Abstract volume, 639-642, Lerida.

Puigdefàbregas C. & Souquet P. (1986) - Tectonosedimentary cycles and depositional sequences of the Mesozoic and Tertiary from the Pyrenees. *Tectonophysics*, 129: 173-203, Berlin Heidelberg.

Remacha, E., Fernández, L.P., Maestro, E., Oms, O. & Estrada R. (1998). The Upper Hecho Group turbidites and their vertical evolution to deltas (Eocene, South-Central Pyrenees). In: Melendez Hevia A. & Soria A. (Eds) – *15th IAS International Sedimentological Congress Field Trip Guidebook*, April 8-12 1998, 1-25, Alicante.

Røe S.L. (1987) - Cross-strata and bedforms of probable transitional dune to upper-stage plane-bed origin from a Late Precambrian fluvial sandstone, northern Norway. *Sedimentology*, 34: 89-101, Oxford.

Saunderson H. & Lockett F.P.J. (1983) - Flume experiments on bedforms and structures at the dune-plane bed transition. In: J.D. Collinson & J. Lewin (Eds) - Modern and ancient fluvial systems, *IAS Spec. Publ. 6*, Blackwell, 49-58, London.

Seguret M. (1972) - Etude téctonique des nappes et séries décollées de la partie centrale du versant-sud des Pyrénées: caractère synsédimentaire, role de la compression et de la gravité. Ph.D. Thesis, University of Montpellier, V. of 155 pp., Montpellier.

Soler M. & Puigdefàbregas C. (1970) - Lineas generales de la geologia del alto Aragon occidental. *Pirineos*, 96: 5-12, Jaca.

Serra-Kiel J., Canudo J.I., Dinares J., Molina E., Ortiz N., Pascual J.O., Samso J.M. & Tosquella J. (1994) - Cronoestratigrafia de los sedimentos marinos del terciario inferior de la Cuenca de Graus-Tremp (Zona Central Surpirenaica). *Rev. Soc. Geol. España*, 7: 273-297, Madrid.

Sohn Y.K., Rhee C.W. & Kim B.C. (1999) - Debris flow and hyperconcentrated flood-flow deposits in an alluvial fan, Northwestern part of the Cretaceous Yongdong Basin, Central Korea. *J. Geol.*, 107: 111-132, Chicago.

Teixell A. (1996) - The Ansò Transect of the southern Pyrenees: basement and cover thrust geometries. *J. Geol. Soc. London*, 153: 301-310, London.

Tinterri R. (1997) - Il problema dell'interpretazione dell'hummocky cross-stratification*. Proceedings, Annual Meeting Italian Sedimentology Group CNR*, 13-17 october 1997, 76-78, Arcavacata di Rende.

Tinterri R. (1999a) - Sedimentologia e stratigrafia fisica dei depositi di barra di foce e lobi di piattaforma della successione eocenica del bacino di Tremp-Graus nell'area della Val Isabena (Pirenei Centro-meridionali). Ph.D. Thesis, University of Bologna, V. of 92 pp., Bologna.

Tinterri R. (1999b) - Relazione tra l'idrogramma di piena e le sequenze di facies di foce (barre) e di piattaforma (lobi). Proceedings Annual Meeting, Italian Sedimentology Group, CNR, Rimini, October 3-6, 1999, *Giornale di Geologia*, 61: 97-100, Bologna.

Tinterri R. (2006a) - The relationship between flood hydrograph and facies sequences of delta-front sandstone lobes produced by hyperpycnal flows. *Proceedings Annual Meeting, Italian Sedimentology Group GEOSED*, Modena 25-29 september 2006, 112, Modena.

Tinterri R. (2006b) - Proposal for a classification scheme for combined flow sedimentary structures and the meaning of sigmoidal- and hummocky-cross stratification in facies analysis. *Proceedings Annual Meeting, Italian Sedimentology Group GEOSED*, Modena 25-29 september 2006, 111, Modena.

Todd S.P. (1989) - Stream-driven, high-density gravelly traction carpets: possible deposits in the Trabeg Conglomerate Formation, SW Ireland and some theoretical considerations of their origin. *Sedimentology*, 36: 513-530, Oxford.

Torricelli S., Knezaurek G. & Biffi U. (2006) - Sequence biostratigraphy and paleoevironmental recostruction in the early Eocene Figols Group of the Tremp-Graus Basin (south central Pyrenees, Spain). *Paleogeogr., Paleoclim. Paleoecol.*, 232: 1-35, Amsterdam.

Vincent S.J. (2001) - The Sis paleovalley: a record of proximal fluvial sedimentation and drainage basin development in response to Pyrenean mountain building. *Sedimentology*, 48: 1235-1276, Oxford.

Waehry A. (1999) - Facies analysis and physical stratigraphy of the Ilerdian in the eastern tremp-Graus basin (south-central Pyrenees, Spain). *Terre et Environments*, 15, XIII, V. of 191 pp., Geneve.

Wright L. D. (1977) - Sediment transport and deposition at river mouths: A synthesis. *Geol. Soc. Am. Bull.*, 88: 857-868, Boulder.

Wright L.D. & Coleman J.M. (1974) - Mississippi river mouth processes: effluent dynamics and morphologic development. *J. Geol.,* 82: 751-778, Chicago.

Wright L.D., Yang Z.S., Bornhold B.D., Keller G.H., Prior D.B. & Wiseman JrW.J. (1986) - Hyperpycnal plumes and plume fronts over the Huanghe (Yellow River) delta front. *Geo-Marine Letters*, 6: 97-105, Berlin Heidelberg.

Wells S.G. & Harvey A.M. (1987) - Sedimentologic and geomorphic variations in storm-generated alluvial fans, Howgill Fells, northwest England. *Geol. Soc. Am. Bull.*, 98: 182-198, Boulder.

Wheatcroft R.A. (2000) - Oceanic flood sedimentation: a new perspective. *Continental Shelf Research*, 20: 2059-2066, Amsterdam.